THE NADPH OXIDASE NOX4 RESTRICTS THE REPLICATIVE LIFESPAN OF HUMAN ENDOTHELIAL CELLS

Running title: Nox4 in replicative senescence

Barbara Lener[1,2]*, Rafał Kozieł[1]*, Haymo Pircher[1], Eveline Hütter[1], Ruth Greussing[1], Dietmar Herndler-Brandstetter[1], Martin Hermann[3], Hermann Unterluggauer[1], and Pidder Jansen-Dürr[1,2$]

[1]Institute for Biomedical Aging Research, Austrian Academy of Sciences, Rennweg 10, A-6020 Innsbruck, Austria
[2]Tyrolean Cancer Research Institute, Innrain 66, A-6020 Innsbruck, Austria
[3]KMT Laboratory, Department of Visceral, Transplant and Thoracic Surgery, Center of Operative Medicine, Innsbruck Medical University, Innrain 66, A-6020 Innsbruck, Austria

* These two authors contributed equally to this work

[$]Address correspondence to: Dr. Pidder Jansen-Dürr, Institute for Biomedical Aging Research, Rennweg 10, A-6020 Innsbruck, Austria, Phone: +43-512-583919-44, FAX: +43-512-583919-8, email: p.jansen-duerr@oeaw.ac.at

Abbreviations footnote:
NOX, NADPH oxidase; ROS, reactive oxygen species; HUVEC, human umbilical vein endothelial cells; SOD, superoxide dismutase; SIPS, stress-induced premature senescence; HDF, human diploid fibroblasts; SA-β-gal, senescence-associated-β-galactosidase; DNPH, 2,4-dinitrophenylhydrazine; DPI, diphenyliodinium; BrdU, bromodeoxyuridine; kb, kilobases

SYNOPSIS

The free radical theory of ageing proposes that reactive oxygen species (ROS) are major driving forces of ageing, and are also critically involved in cellular senescence. Besides the mitochondrial respiratory chain, alternative sources of ROS have been described, which might contribute to cellular senescence. NADPH oxidases are well-known sources of superoxide, which contribute to the antimicrobial capabilities of macrophages, a process involving the prototypical member of the family referred to as Nox2. However, in the recent years non-phagocytic homologues of Nox2 have been identified, which are involved in processes other than the host defence. Superoxide anions produced by these enzymes are believed to play a major role in signalling by MAP kinases and stress-activated kinases, but could also contribute to cellular senescence, which is known to involve oxygen radicals. In human umbilical vein endothelial cells (HUVEC), Nox4 is predominantly expressed, but its role for replicative senescence of HUVEC remains to be elucidated. Using shRNA-mediated knockdown of Nox4, implicating lentiviral vectors, we addressed the question if lifelong depletion of Nox4 in HUVEC would influence the senescent phenotype. We found a significant extension of the replicative lifespan of HUVEC upon knockdown of Nox4. Surprisingly, mean telomere length was significantly reduced in Nox4-depleted cells. Nox4 depletion had no discernable influence on the activity of MAP kinases and stress-activated kinases, but reduced the degree of oxidative DNA damage. These data suggest that Nox4 activity increases oxidative damage in HUVEC leading to loss of replicative potential which is at least partly independent of telomere attrition.

Key Words:
Nox4 / replicative senescence / HUVEC / DNA damage / telomere attrition / oxidative stress

INTRODUCTION

The free radical theory of ageing considers molecular damage caused by the presence and action of reactive oxygen species (ROS) as a major cause for ageing processes in most if not all species. The role of ROS as mediators of senescence and determinants of lifespan has been addressed by genetic studies in several model organisms (for review, see ref. [1]). Thus, reducing the level of antioxidant enzymes such as superoxide dismutase (SOD), leads to a consistent reduction of the lifespan in many species, including the mouse [2]. Accordingly, extending the antioxidative capacity, for example by overexpression of SOD/catalase [3] has been shown to extend lifespan in an otherwise short-lived strain of the fruitfly *D. melanogaster*, whereas ectopic overproduction of mitochondrial catalase can prolong the lifespan of mice [4]. However, there are also examples where overexpression of antioxidant enzymes did not extend the lifespan; thus, a large cohort study demonstrated that overexpression of CuZnSOD does not increase lifespan of the mouse [5]; similarly, catalase-transgenic mice are not long-lived but rather display enhanced sensitivity to oxidative stress [6]. Whereas these data support the concept that ROS-induced damage contributes to ageing processes, at least in some specific genetic backgrounds, the role of the individual antioxidant enzymes in this process remains to be determined.

Concerning human ageing, many questions about molecular mechanisms have been addressed using *in vitro* senescence models derived from normal human cells. The proliferative potential of human primary cells in culture is limited, and extended passaging of such cells leads to a state of terminal growth arrest, referred to as replicative senescence. While the erosion of telomeres, due to insufficient telomerase activity (for recent review, see [7]), has been recognized as a primary cause of replicative cellular senescence, a variety of other events have been identified that trigger premature senescence. Most notably, oxidative stress was found to induce premature senescence in human fibroblasts [8, 9], endothelial cells [10, 11], and a variety of other cell types (reviewed in ref. [12]).

The mitochondrial theory of ageing [13] suggests a critical role for mitochondrial dysfunction and subsequently increased ROS production as an inducer of ageing and premature senescence. Accordingly, replicative senescence of human diploid fibroblasts (HDF) has been associated with mitochondrial dysfunction and mitochondrial ROS were identified as important players in the senescence response of HDF [14-16]. However, mitochondrial dysfunction does not seem to be uniformly responsible for senescence in all cell types. In particular, the role of mitochondrial dysfunction in senescence of human umbilical vein endothelial cells (HUVEC) has remained controversial. Depending on the particular strain of HUVEC and the techniques applied to assess mitochondrial function, one can observe a wide range of effects, ranging from serious mitochondrial dysfunction [17] to no effect at all [18], suggesting that other cellular ROS sources may contribute to the senescent phenotype.

NADPH oxidases generate superoxide, which, together with its derivatives, fulfills diverse intracellular functions. Notably, superoxide production by phagocytes and macrophages is activated in response to bacterial or viral infections. This process, characterized by rapid activation of the phagocytic enzyme Nox2, is referred to as oxidative burst [19]. In addition, non-

phagocytic members of the NADPH oxidase (Nox) gene family have recently been identified. Of those, Nox1 plays a role in the host defence (reviewed in ref. [20]), whereas other Nox family members are known to play a role in signal transduction [21]. Based on both, overexpression and gene-knockdown experiments, it has been shown that Nox1 triggers the activation of JUN kinase (JNK) by phosphorylation [22]. For Nox4, it has been shown that knockdown leads to decreased MAP kinase activity in various cell types [23, 24] and Nox4-induced activation of p38 was shown to drive differentiation of murine cardiomyocytes [25]. Nox4 knockdown in pancreatic cancer cells down-regulated the activity of protein kinase B/AKT [26]. Whereas Nox4 was shown to stimulate the proliferation of various cell types, it was also shown to promote differentiation and restrict cell proliferation ([27-29], for recent review, see ref. [30]). Whereas these observations indicate that Nox4 has the potential to modulate the proliferative capacity of various cell types in several ways, the role of NADPH oxidases in replicative senescence of human cells has not been explored so far. Given the implication of Nox4 in ROS production and cellular signalling pathways, we addressed the possibility that Nox 4 may be involved in replicative senescence of human endothelial cells.

EXPERIMENTAL

Cell Culture

Endothelial cells of four different donors were isolated from human umbilical veins and maintained in Endothelial Cell Medium (Cambrex BioScience), as described [10]. To achieve maximal viability, cells were grown on dishes pre-coated with gelatine (0.1% in Endothelial Cell Medium; Sigma- Aldrich) [31]. Cells were counted when passaged and population doublings (PDL) were estimated using the following equation: n = (log10F - log10I) / 0.301 (n represents the number of population doublings, F the number of cells at the end of one passage and I the number of cells that were seeded at the beginning of one passage). Depending on the donor, cells reached senescence after different numbers of population doublings.
For production of lentiviral particles, HEK-T cells were maintained in DMEM, containing 2 mM L-glutamine, 100 U/ml Penicillin, 0.1 mg/ml Streptomycin and 10% fetal bovine serum (heat inactivated).

Lentiviral infection of HUVEC cells

Production of lentiviral particles was carried out according to the manufacturer's protocol (Addgene Inc.) by usage of the packaging plasmids pMD2.G and psPAX2 (both purchased from Addgene Inc.) and the lentiviral vector pLKO.1, containing Nox4-specific shRNA and control shRNA, respectively (Open Biosystems). For lentiviral infection, HUVEC cells of early passage were cultivated in 6-well plates. Upon reaching ~70% confluence, culture medium, containing lentiviral particles to the amount of 2 MOI, was added to the cells in presence of 8 µg/ml hexadimethrine bromide (Sigma-Aldrich), which increases the efficiency of viral infection. 24h after infection, medium was changed. Puromycin selection was initiated (500 ng/ml) 48h post infection.

Staining for senescence- associated ß-galactosidase (SA-ß-gal)

The senescent status of the cells was monitored by *in situ* staining for SA-ß-galactosidase, as described [10].

PCR-based quantification of mRNA levels

For semiquantitative reverse-transcription-PCR (RT-PCR), total RNAs were isolated from cells using the 'RNeasy Mini' kit (Qiagen). 1 µg of total RNA was applied to reverse transcription using the 'Transcriptor First Strand cDNA Synthesis Kit' (Roche Applied Science) and oligo(dT) primer. Follow-up PCR amplification of Nox4 mRNA was carried out using suitable primers, whereas ß- actin served as loading control.
For quantitative Real-Time PCR (qPCR), primers for the detection of Nox4 mRNA and the housekeeper gene porphobilinogen deaminase (PBGD) were designed using Primer3 software, as follows:

5'-AGTCCTTCCGTTGGTTTG-3' (fwd) and 5'-AAAGTTTCCACCGAGGAC-3' (rev) for Nox4- amplification as well as 5'-CCAGGACATCTTGGATCT-3' (fwd) and 5'-ATGGTAGCCTGCATGGTCTC-3' (rev) for PBGD amplification.. Total RNA was isolated and used for reverse transcription, as previously described [32]. The cDNA equivalent of 5 ng RNA was applied to PCR amplification in combination with 15 µl of 'LightCycler® 480 SYBR Green I Master' (Roche Applied Science), a reaction mixture, including FastStart Taq DNA Polymerase and SYBR Green I dye for product detection. cDNA concentrations were normalized by the use of the internal standard PBGD. Real-Time PCR was performed in triplicates in the LightCycler® 480 Instrument (Roche Applied Science) in a final reaction volume of 50µl per tube. Cycling conditions were as follows: 95°C for 8min (initial denaturation step) followed by 55 cycles of target amplification (95°C for 15sec, 57°C for 8sec, and 72°C for 15sec) and final melting (95°C for 1min, 60°C for 30sec, 95°C continuous with 5 acquisitions per °C).. Crossing Points (Ct) for Nox4 and PBGD in control cells / shRNA- treated cells were used for calculation of Nox4 fold expression changes.
Absolute quantification of Nox4 expression in different HUVEC isolates was based on a dilution range of an external plasmid standard to obtain a standard curve (Ct values of the standard versus gene copy numbers). Ct values for Nox4 in HUVEC samples were extrapolated against this plot in order to calculate absolute copy numbers of Nox4 mRNA.

Determination of ROS production by chemiluminescence

Reactive oxygen species were detected by luminol-enhanced chemiluminescence. The assay was performed in 24-well format. Cells were seeded in order to reach 80-90% confluency after 24 h. The following day, cells were washed once with HBSS (Sigma-Aldrich). Afterwards, 1.0 ml of HBSS (containing 10 µg/ml Luminol and 4U/ml Horseradish Peroxidase, both purchased from Sigma-Aldrich) was added to each well. Cells were incubated at 37°C in a multiple plate reader (HIDEX CHAMELEON, HVD) and ROS production was monitored over a period of 20 - 25min by recording light emission (luminescence). Diphenyliodonium (DPI; 10 µM; Sigma-Aldrich) was added towards the end of the measurement to abolish Nox-dependent ROS production. The luminescence signal (expressed in relative light units, RLUs) was normalized to cell number.

BrdU staining for quantification of cell proliferation

DNA synthesis was assessed using the '5-Bromo-2'-deoxy-uridine Labeling and Detection Kit I' (Roche Applied Science) according to the manufacturer's recommendations for adherent cells. After the staining procedure, the coverslips were analyzed by fluorescence microscopy. Cells of 3 visual fields were counted and the number of BrdU-positive cells was expressed as percent of the total cell number.

Standard immunoblotting analysis

Cellular protein lysates were prepared on ice in RIPA buffer containing protease- and phosphatase- inhibitors. Lysates were centrifuged and protein concentration in the resulting supernatants was determined, using the 'Detergent Compatible Assay' (DC Protein Assay;

BioRad). Appropriate amounts of protein were subjected to SDS gel electrophoresis (10% SDS/polyacrylamid gels) and transferred to PVDF membranes. Membranes were blocked with 5% BSA in TBS / 0.1% Tween20 and incubated with primary antibodies overnight. Proteins of interest were detected after incubation with horseradish peroxidase-conjugated secondary antibodies (Dako Cytomation) and visualized with enhanced chemoluminiscence reagent ECL (Amersham). Used antibodies were as follows: anti-Phospho ERK1,2 (New England Biolabs), anti-Phospho JNK (New England Biolabs), anti-Phospho p38 (Cell Signalling), anti-ERK1,2 (Santa Cruz), anti-JNK1 (Santa Cruz), anti-p38 (Cell Signalling), and anti-alpha Tubulin (Sigma-Aldrich). Results (signal intensities) from three independent experiments were subjected to densitometric analysis using AlphaEaseFC software..

Preparation and fractionation of cell lysates for Nox immunoblotting

Transfected U-2OS cells were scraped off 10 cm Petri- dishes and afterwards recollected in 900 µl PBS containing protease inhibitors (Roche, Complete, EDTA-free) kept on ice. Cell lysis was achieved by freeze-thaw cycles and sonication. After centrifugation, the supernatant containing soluble proteins was mixed with standard SDS-PAGE sample buffer and boiled for 5 min. The insoluble pellet was resuspended in membrane protein extraction buffer (20 mM MOPS pH 7.2, 2% Triton X-100, 0.5 M NaCl, 0.25 M sucrose), sonicated, and centrifuged. The supernatant was mixed with an equal volume of membrane protein sample buffer (10% SDS, 3% ß-mercaptoethanol, 15% glycerol, 0.025% bromphenol blue, 75 mM Tris-HCl pH 7.0) and incubated at 40°C for 30 min. Soluble and membrane protein fractions were then analyzed by SDS-PAGE and subsequent Western blotting. For detection of Nox4, the antibodies anti-Nox4 sc30141 (Santa Cruz Biotechnology) and anti-Nox4 NB110-58849SS (Novus Biologicals) were used. We further applied an affinity-purified goat antiserum obtained against the C-terminal part of Nox4, which was expressed in *E.coli* and purified to homogeneity (H. Pircher, unpublished).

Analysis of oxidative damage to DNA

Flow-cytometric detection of 8-oxodeoxyguanosine was performed according to ref. [33]. Briefly, the cells grown on ~90% confluent 10 cm Petri-dishes were collected and resuspended in PBS. For fixation, formaldehyde was added to the final concentration of 2.5% and the cells were incubated for 10 min at 37°C. Cells were chilled on ice for 1 min, rinsed by centrifugation and permeabilized by addition of 90% ice-cold methanol. After 30 minutes incubation on ice, 0.5 – 1 $\times 10^6$ cells were aliquoted into each assay tube and washed twice with PBS. After centrifugation (800 × *g*, 5 min), cell pellets were blocked for 10 minutes at room temperature in 300 µl PBS containing 10 % (w/v) normal goat serum (NGS). After two washing steps with PBS containing 0.2 % (w/v) NGS, the cells were stained in 200 µl avidin-conjugated FITC solution (Sigma, A2050), resuspended 1:200 in PBS and incubated for 1h at room temperature. After two washings with PBS, cells were resuspended in 400 µl PBS and analyzed by flow cytometry. As a negative control, cells incubated in the absence of avidin-conjugated FITC were used.

Detection of DNA double-strand breaks by gamma-H2AX staining

To detect phosphorylation of the histone H2A variant, H2AX, at Serine 139, which generates γ-H2AX, a well-established marker of DNA double-strand breaks [34], flow cytometry as well as immunofluorescence procedures were carried out, using anti- γ-H2AX antibody (Cell Signaling, #2577), according to the protocols provided by the manufacturer. In both cases, anti-γ-H2AX antibody, diluted 1:50, and a FITC-conjugated swine anti-Rabbit Ig secondary antibody (Dako, #F0205), diluted 1:20, were used. As positive control, cells incubated for 1h at room temperature with 100 µM H_2O_2 in HBSS were used. As negative control, cells incubated in the absence of primary antibody were used. Staining of the cells was analyzed by confocal microscopy using a microlens-enhanced Nipkow disk-based confocal system UltraVIEW RS (Perkin Elmer, Wellesley MA, USA) mounted on an Olympus IX-70 inverse microscope (Olympus, Nagano, Japan). Images were acquired using a 100 x oil immersion objective (Olympus, PlanApo, NA 1,4).

Determination of mean telomere length

For flow cytometric analysis of the mean telomere length, a modified protocol based on ref. [35] was used. Briefly, 1×10^6 cells grown on 10 cm Petri-dishes (~90% confluent) were transferred into FACS tubes and washed once with PBS. After centrifugation (400 × *g*, 10 min), cells were resuspended in 1 ml hybridization buffer (49% formamide, 1% BSA, 20 mM Tris-HCl, pH 7.2) and rinsed by centrifugation (1000 × *g*, 10 min). The cells were then resuspended in 96.25 µl hybridization buffer and PNA probe (PNA probe TelC-FITC, Panagene #080506PL-14) was added to the final concentration of 375 nM. After the incubation step (12 min at 85°C), the tubes were chilled on ice for 2 min and incubated for 90 min at room temperature in the dark. The cells were washed twice with 2 ml post-hybridization buffer (49% formamide, 0.1% BSA, 0.1% Tween-20, 10 mM Tris-HCl, pH 7.2) and rinsed by centrifugation (1000 × *g*, 10 min). The cells were then washed twice with PBS (1000 × *g*, 10 min) and resuspended in 300 µl PBS. Cell suspensions were subjected to flow cytometry using a FACSCanto™ II (BD Biosciences). The mean fluorescence intensity (detector FL1) was used to estimate relative telomere length. Human TCL 1301 cells, displaying a relatively constant mean telomere length of roughly 25 kb [35], served as a reference. As a negative control, sample without PNA probe was used.

RESULTS

Expression and activity of NADPH oxidases in young and senescent HUVEC

To determine mRNA levels of NADPH oxidases in young and senescent HUVEC, RNA was prepared from 4 different HUVEC isolates, which were either harvested at early passage (passage 3) or harvested after extended passaging when cells reached senescence (around passage 25). As described before [32], there is a certain variation in the phenotype between HUVEC strains isolated from different donors. This is also reflected by the fact, that the proliferative capacity of the 4 different isolates examined, varied between 45 (e.g. HUVEC strain #1) and 55 (e.g. HUVEC strain #3) population doublings (PDL) before the cultures reached senescence. Data obtained by RNA profiling using Affymetrix^{TM} microarrays indicated that, despite the phenotypical variation noted above, a conserved pattern of gene expression can be observed upon senescence in various HUVEC strains (unpublished results). Expression levels of Nox1, 2, 3 and 5 were rather low in young HUVEC, and no significant senescence-associated changes in the expression of these genes were observed. However, in all strains a signal for Nox4 was readily detectable by both methods, RT-PCR and quantitative Real Time-PCR (qPCR). For all HUVEC strains analyzed, the level of Nox4 mRNA was virtually unaltered when young and senescent cultures of HUVEC were compared (Fig. 1A, and data not shown). Using RT-PCR, we also detected expression of $p22^{phox}$, the only known additional subunit required for Nox4 activity (reviewed in ref. [36]), in all HUVEC strains (data not shown).

To assess the rate of Nox-derived ROS production, luminol-enhanced chemiluminescence was applied, which is a convenient and sensitive assay to determine cell-associated NADPH oxidase activity [37]. Using human osteosarcoma cells (U-2OS) stably transfected with expression vectors for both, Nox4 and $p22^{phox}$, we confirmed luminol-enhanced chemiluminescence to be a valid method for measuring Nox4-derived ROS, since double-transfected U-2OS cells yielded a robust signal, whereas untransfected U-2OS cells, which lack both enzymatic compounds, yielded no signal in this assay (data not shown). Chemiluminescence signals were quenched more than 90% upon addition of DPI, further supporting our consideration of the assay being specific for detection of NADPH oxidase activity . Similar results were obtained upon incubation of Nox4-expressing U-2OS cells with the redox-sensitive probe Amplex Red (data not shown), which represents another assay frequently used to detect Nox activity, preferably by measuring extracellular hydrogen peroxide [38].

Significant chemiluminescence signals were detectable in case of all HUVEC strains at early passage. Signals were efficiently quenched upon the addition of the NADPH oxidase inhibitor diphenyliodonium (DPI) (Fig. 1B), indicating a significant contribution of NADPH oxidase activity to overall ROS production in HUVEC. Nox activity was also detectable in cells of senescent cultures, although the activity per cell was somewhat lower in senescent cells of all strains (Fig. 1B, and data not shown).

Inactivation of Nox4 enhances cell proliferation in HUVEC.

To address the growth-modulating potential of Nox4 in HUVEC, we applied lentiviral vectors for delivery of Nox4-specific shRNA. Lentiviral particles are known to efficiently infect HUVEC [32]. Infections were performed in cells of HUVEC strains #1 and #3 at early passage (p5), and cells were grown under puromycin selection to ensure efficient knockdown in all cells. 42 days after infection, RNA was harvested and analyzed by qPCR. This experiment revealed a significant (7-12 fold) downregulation of Nox4 mRNA in the case of Nox4-specific shRNA, whereas control shRNA showed no effect (Fig. 2A).

We also attempted to analyze Nox4- knockdown at the protein level by Western blot analysis, which, due to the limited availability of immunological reagents, has been notoriously difficult (reviewed in ref. [39]). To assess the quality of the immunological reagents available to us, U-2OS osteosarcoma cells were transfected with Nox4 expression vectors. Since NADPH oxidases are membrane-bound enzymes, we applied a specific protocol for cell lysis which ensures efficient solubility of membrane proteins which under normal lysis conditions would remain undetectable [40]. As control for the lysis procedure, the related protein Nox5 was used, against which high quality antibodies (a gift from Karl-Heinz Krause) have been created . Nox5 was easily detectable in these experiments (Fig. S1), thereby validating our experimental protocol for the detection of Nox enzymes by Western blot analysis. Whereas a commercially available antibody to Nox4 as well as an affinity-purified goat antiserum, directed against the C-terminal part of Nox4 (H. Pircher, unpublished), detected weak but significant signals in the membrane fraction of Nox4- transfected cells (Fig. S1), the sensitivity of both antibodies was not sufficient to detect endogenous Nox4 in untransfected HUVEC (data not shown), which precluded the analysis of Nox4-knockdown in HUVEC by Western blot. However, expression of Nox4-specific shRNA led to an almost complete suppression of NADPH oxidase activity, assessed by luminol-enhanced chemiluminescence (Fig. 2B). Chemiluminescence signals were quenched more than 90% upon addition of DPI (data not shown). Together, these data strongly suggest Nox4 being the functionally relevant Nox isoform in HUVEC.

To determine whether Nox4 depletion affects the rate of cell proliferation, bromodeoxyuridine (BrdU) incorporation studies were performed. As for the parental HUVEC strains, cells derived from strain #3 through infection with control shRNA showed a slightly higher rate of BrdU incorporation (19+/- 3%; Fig. 3A), compared to strain #1 (14 +/- 1.5%; Fig. 3A), reflecting the higher proliferative activity of HUVEC strain #3 (data not shown). In both HUVEC strains, expression of Nox4-specific shRNA led to a significant increase in the rate of cell proliferation, as shown by BrdU incorporation (Fig. 3A). It is known that Nox4 activity plays an important role in specific signal transduction processes which can modulate cell proliferation, such as signalling through ERK1/2 [24] and stress-activated kinase p38 [25], whereas Nox1 is known to mediate activation of JUN kinase (JNK) in vascular smooth muscle cells [22]. To investigate whether signalling through these pathways is affected by Nox4 gene knockdown in HUVEC, the expression and activation state of these kinases was determined. Extracts were prepared from HUVEC that had been either infected with control shRNA or Nox4-specific shRNA, and probed with antibodies to ERK1/2, JNK and p38. To assess the activation status of the respective kinases, we used phosphorylation-specific antibodies directed against phospho-ERK, phospho-JNK and phospho-p38, respectively. Whereas in control experiments, using human diploid

fibroblasts that were either growth arrested by serum starvation for 72 hours, or stimulated with 10% FCS, a clear-cut activation of both ERK and p38 was visible, no significant changes in these signalling pathways could be observed in HUVEC transduced with Nox4-specific shRNA. Similarly, control experiments with anisomycin-treated human fibroblasts revealed a clear increase in the levels of phosphorylated JNK, whereas the levels of both, JNK and phospho-JNK, were not significantly affected by Nox4 shRNA (Fig. 3B). Together, these data suggest that downregulation of Nox4 in two independent HUVEC isolates did not significantly affect the activity of the three protein kinases studied (Fig. 3C).

Inactivation of Nox4 delays HUVEC replicative senescence.

To study the role of Nox4 in replicative senescence of HUVEC, early-passage cells of both strains, #1 and #3 were subjected to lentiviral infection, with particles harbouring control shRNA or Nox4-specific shRNA, and grown into senescence. Efficient and persistent knockdown of Nox4 was confirmed by qPCR (Fig. 4A) and luminol-enhanced chemiluminescence (data not shown). Cell proliferation was assessed by cell counting at every passage, thereby cumulated population doublings (cPDL) were calculated. We found that shRNA-mediated knockdown of Nox4 led to a significant extension of the population doubling capacity in both HUVEC strains #1 (Fig. 4B) and #3 (Fig. 4C). Accordingly, the relative proportion of cells, that stained positive for SA-ß-gal activity was significantly reduced upon transfection with Nox4-specific shRNA (Fig. 4D).

Replicative senescence is known to be triggered primarily by telomere shortening (for recent review, see [7]), although it is known that other processes, such as oxidative stress, can shorten the cellular lifespan as well [10, 11, 41]. To elucidate the role of telomere shortening in context with the observed lifespan extension in response to Nox4 depletion, telomere length was determined in Nox4-depleted cells as well as in control cells. Telomere length was estimated by Flow FISH [42], using telomeres of a stable T cell line as size marker [35]. The mean telomere length of HUVEC was gradually reduced through extended passaging to a minimal length of roughly 20 kb, when cells reached senescence (data not shown; see also ref. [43]). This finding is in agreement with the observations of others who reported telomere shortening to be a key mechanism of cellular senescence in HUVEC [11]. When the influence of Nox4 knockdown on mean telomere length was analyzed, we found that the mean telomere length of 22 kb in control cells of strain #3 at passage 15 was reduced to 13 kb in case of Nox4-depleted cells of the same strain. Similarly, telomere length of 28 kb in control cells of strain #1 at passage 17 was reduced to 18 kb in Nox4-depleted cells of the same strain (Fig. 5). These findings suggest that depletion of Nox4 extends the proliferative capacity of HUVEC, resulting in a decreased mean telomere length in Nox4-depleted cells.

Inactivation of Nox4 delays the accumulation of oxidative damage

The data obtained so far suggest that Nox4 contributes to replicative senescence of HUVEC. ROS-induced damage to nucleic acids (reviewed in ref. [16]) and proteins [44] is believed to contribute to cellular senescence, and our data raise the possibility that in HUVEC, ROS

produced by Nox4 may be involved in this process. Accordingly, the observed delay of senescence in Nox4-deficient HUVEC may be due to reduced oxidative damage, otherwise affecting cellular constituents, such as DNA and proteins. To test this hypothesis, the degree of DNA damage was determined by quantification of 8-oxodeoxyguanosine (8 oxo-dG), an established marker of oxidative DNA damage [33]. To this end, HUVEC strains #1 and #3, infected with either control shRNA or Nox4-specific shRNA, were stained with avidin-FITC, a well-established and specific ligand for 8 oxo-dG [33]. Fluorescence intensities were analyzed by flow cytometry. This experiment revealed a significant reduction of 8 oxo-dG content in Nox4- knockdown cells (Fig. 6A).

To further characterize Nox4-derived DNA damage, cells were stained with antibodies to γ-H2AX and analyzed by indirect immunofluorescence. Histone variant H2AX is phosphorylated in response to DNA double-strand breaks to yield γ-H2AX, which is recruited to sites of DNA damage [34]. We detected specific nuclear γ-H2AX staining in control cells (transfected with control shRNA), which was markedly reduced in Nox4-depleted cells (Fig. 6B). In both cell types, γ-H2AX staining was enhanced upon treatment with H_2O_2, providing a control for the staining assay. γ-H2AX staining intensity was quantified using flow cytometry (Fig. 6C), which confirmed significantly reduced fluorescence in case of Nox4-depleted cells. DNA damage is known to initiate antiproliferative signals and contribute to senescence in several models of senescence *in vitro* (reviewed in ref. [45]) and probably also *in vivo* (reviewed in ref. [46]). Together, these data suggest that Nox4-derived ROS induce DNA damage in HUVEC, thereby leading to the establishment of cellular senescence.

DISCUSSION

The occurence of reactive oxygen species (ROS), originating from the mitochondrial electron transport chain, is upregulated with age in many species including humans, and solid evidence suggests that mitochondria-derived ROS mechanistically contribute to ageing in a variety of experimental model systems. Concerning the *in vitro* senescence of human diploid fibroblasts, it has been demonstrated that mitochondrial dysfunction and increased ROS production are tightly linked in senescent cells, and it is now widely accepted that dysfunctional mitochondria play a key role in fibroblast senescence. Concerning human endothelial cells, the link between senescence and mitochondrial dysfunction is less clear, raising the possibility that other ROS sources could contribute to senescence of human endothelial cells. To address the question if NADPH oxidases play a role in the senescence response of human umbilical vein endothelial cells (HUVEC), we have analyzed the expression pattern of Nox genes in HUVEC, isolated from four different donors. PCR analysis revealed consistent expression of Nox4 in all four isolates, whereas the expression level of other Nox family members was rather low. To assess the influence of Nox4 on the replicative potential of these cells, shRNA-encoding vectors were used for sustained depletion of Nox4 in HUVEC. Nox4 knockdown enhanced the rate of cell proliferation and resulted in a significant extension of cellular lifespan, consistent with the model that Nox4-derived ROS contribute to the onset of replicative senescence in human endothelial cells.

Role of Nox enzymes in signal transduction and cell proliferation in HUVEC.

RT-PCR analysis revealed Nox4 to be the major NADPH oxidase isoform in four different HUVEC isolates. In contrast to findings reported by others [47], Nox2 was not detectable at both, mRNA as well as protein level in the HUVEC strains implicated in this study. Similarly, mRNA levels for Nox1, Nox3, and Nox5 were rather low in all four HUVEC isolates (B. Lener, unpublished). Limitations concerning the sensitivity of available antibodies restricts reliable detection of Nox4 protein to cells with high expression levels (Fig. S1). None of the available antibodies was able to detect endogenous Nox4 protein in HUVEC (data not shown). In light of this fact, we chose to assess cellular ROS production to determine the efficiency of shRNA-mediated Nox4 depletion. Using U-2OS cells stably transfected with both, Nox4 and $p22^{phox}$ expression vectors, luminol-enhanced chemiluminescence was established as a convenient method to assess Nox4 activity in cells. Using this assay, we found the presence of Nox4 mRNA being closely connected to the presence of elevated ROS production, which could be successfully inhibited by the NADPH oxidase inhibitor DPI. DPI-sensitive ROS production was lost upon shRNA-mediated knockdown of Nox4, supporting our conclusion that the majority of NADPH oxidase activity in HUVEC is due to Nox4.

We found that shRNA-mediated abrogation of Nox4 activity results in increased cellular proliferation. Nox4 is required for proliferation of various cell types [27-29]; on the other hand, Nox4 can also promote differentiation and restrict cell proliferation (reviewed in ref. [30]). These observations indicate that the influence of Nox4 on cell proliferation capacity is cell type-specific and may be further influenced by cell culture conditions. Based on the literature [48, 49],

one would expect that inactivation of Nox4 reduces signalling through ERK1/2 and/or stress-activated kinase pathways. However, we failed to detect any significant decrease in ERK phosphorylation, JNK phosphorylation and p38 kinase phosphorylation, suggesting that the maintenance of those pathways may require relatively low levels of Nox4 activity in HUVEC.

Oxidative stress and cellular senescence: the role of mitochondria and alternative ROS sources.

Employing high-resolution respirometry, we have previously shown that mitochondria are partially uncoupled in senescent human dermal fibroblasts [14], and that experimental uncoupling of mitochondria in young fibroblasts induces premature senescence [15]. In a similar study, mitochondrial dysfunction was observed in senescent human lung fibroblasts and mitochondrial ROS production was identified as one of the causes of replicative senescence in human fibroblasts [16]. A significant increase in oxidative stress was also observed in senescent human endothelial cells [10, 11]; however, the sources for increased ROS production have remained elusive. Depending on the particular strain of HUVEC and the techniques used to assess mitochondrial function, one can observe a wide range of effects, ranging from serious mitochondrial dysfunction [17] to no effect at all [18]. Whereas more work will be required to establish the role of mitochondrial dysfunction in HUVEC senescence, the data presented in this communication indicate that ROS derived from Nox4 play an important role in HUVEC replicative senescence. Lifespan extension linked to Nox4 knockdown could not been observed upon the application of protocols implicating short-term knockdown, via transient transfection with Dharmacon oligonucleotides (H. Pircher, unpublished results). The occurence of the effects described requires lifelong depletion of Nox4, which can only be obtained using lentiviral vectors. We think that the influence of Nox4 activity on lifespan is based on a continuous accumulation of reactive oxygen species and oxidative damage, starting already at early passage. In this respect, it is conceivable that Nox4-derived ROS, in addition to their role as signalling molecules, induce damage to cellular constituents, such as DNA and proteins. This idea is supported by our finding that knockdown of Nox4 resulted in a drastic reduction of DNA damage (Fig. 6), which was accompanied by reduced levels of protein damage, determined as protein carbonyls (data not shown). This finding suggests that reactive oxygen species produced by Nox4 may contribute to lifespan restriction caused by accumulation of damaged DNA (and proteins).

Surprisingly, HUVEC infected with control shRNA underwent senescence-associated growth arrest with relatively high mean telomere length (roughly 20 kb; unpublished), whereas Nox4-depleted HUVEC were still proliferating with significantly shorter telomeres (e.g. 13 kb in HUVEC strain #3, see Fig. 5), suggesting that growth arrest in normal HUVEC may be at least in part telomere-independent. Others have shown that overexpression of Nox4 results in the induction of a senescence-like growth arrest in immortalized murine fibroblasts [50], and that angiotensin II accelerates the onset of senescence in endothelial progenitor cells [51], probably by stimulating Nox2 activity [52]. Whereas overexpression of a foreign gene in an immortalized cell line does not necessarily reveal the physiological role of the gene in question, the approach chosen by us, namely to deplete cells of endogenous Nox4, seems more suitable to reveal its physiological function. When this work was nearly finished, Schilder et al. reported that chronic

incubation of HUVEC with the plant-derived polyphenol resveratrol induces a senescence-like phenotype [53]. They further showed, that inhibition of cell cycle progression in resveratrol-treated cells could be alleviated by knocking down Nox1 in short term transient transfections with shRNA; a similar albeit weaker effect was also observed upon shRNA-mediated knockdown of Nox4. In this study, depletion of either Nox4 or Nox1 had no effects on the phenotype of wild-type HUVEC in the absence of resveratrol [53]. It is conceivable that this observation, which contrasts with our current finding that Nox4 knockdown significantly extends HUVEC lifespan, reflects inefficient knockdown of Nox4 achievable by transient transfection. Therefore the current study, applying lifelong Nox4 depletion in HUVEC in the absence of any pharmacological treatment, demonstrates for the first time that replicative senescence of human endothelial cells can be delayed by reducing endogenous Nox4 activity. Preliminary data from our laboratory suggest that Nox4 knockdown also leads to a moderate lifespan extension in human fibroblasts (R. Greussing et al., unpublished), suggesting a more general role of Nox4 in cellular senescence; however, more work will be required to clarify this point.

ACKNOWLEDGEMENTS

We acknowledge excellent technical support by Michael Neuhaus.

FUNDING

This work was supported by grants from the Austrian Science Funds (NFN S93) and the European Union (Integrated Project MiMage, LSHM-CT-2004-512020). The authors declare no competing financial interest.

REFERENCES

1 Sohal, R. S., Mockett, R. J. and Orr, W. C. (2002) Mechanisms of aging: an appraisal of the oxidative stress hypothesis. Free radical biology & medicine. **33**, 575-586

2 Kokoszka, J. E., Coskun, P., Esposito, L. A. and Wallace, D. C. (2001) Increased mitochondrial oxidative stress in the Sod2 (+/-) mouse results in the age-related decline of mitochondrial function culminating in increased apoptosis. Proceedings of the National Academy of Sciences of the United States of America. **98**, 2278-2283

3 Orr, W. C. and Sohal, R. S. (1994) Extension of life-span by overexpression of superoxide dismutase and catalase in Drosophila melanogaster. Science (New York, N.Y. **263**, 1128-1130

4 Schriner, S. E., Linford, N. J., Martin, G. M., Treuting, P., Ogburn, C. E., Emond, M., Coskun, P. E., Ladiges, W., Wolf, N., Van Remmen, H., Wallace, D. C. and Rabinovitch, P. S. (2005) Extension of Murine Lifespan by Overexpression of Catalase Targeted to Mitochondria. Science (New York, N.Y

5 Huang, T. T., Carlson, E. J., Gillespie, A. M., Shi, Y. and Epstein, C. J. (2000) Ubiquitous overexpression of CuZn superoxide dismutase does not extend life span in mice. The journals of gerontology. **55**, B5-9

6 Chen, X., Liang, H., Van Remmen, H., Vijg, J. and Richardson, A. (2004) Catalase transgenic mice: characterization and sensitivity to oxidative stress. Archives of biochemistry and biophysics. **422**, 197-210

7 Shawi, M. and Autexier, C. (2008) Telomerase, senescence and ageing. Mechanisms of ageing and development. **129**, 3-10

8 Chen, Q. and Ames, B. N. (1994) Senescence-like growth arrest induced by hydrogen peroxide in human diploid fibroblast F65 cells. Proceedings of the National Academy of Sciences of the United States of America. **91**, 4130-4134.

9 von Zglinicki, T., Saretzki, G., Docke, W. and Lotze, C. (1995) Mild hyperoxia shortens telomeres and inhibits proliferation of fibroblasts: a model for senescence? Experimental cell research. **220**, 186-193.

10 Unterluggauer, H., Hampel, B., Zwerschke, W. and Jansen-Durr, P. (2003) Senescence-associated cell death of human endothelial cells: the role of oxidative stress. Experimental gerontology. **38**, 1149-1160

11 Kurz, D. J., Decary, S., Hong, Y., Trivier, E., Akhmedov, A. and Erusalimsky, J. D. (2004) Chronic oxidative stress compromises telomere integrity and accelerates the onset of senescence in human endothelial cells. Journal of cell science. **117**, 2417-2426

12 Colavitti, R. and Finkel, T. (2005) Reactive oxygen species as mediators of cellular senescence. IUBMB life. **57**, 277-281

13 Miquel, J. (1991) An integrated theory of aging as the result of mitochondrial-DNA mutation in differentiated cells. Arch Gerontol Geriatr. **12**, 99-117

14 Hutter, E., Renner, K., Pfister, G., Stockl, P., Jansen-Durr, P. and Gnaiger, E. (2004) Senescence-associated changes in respiration and oxidative phosphorylation in primary human fibroblasts. Biochem J. **380**, 919-928

15 Stockl, P., Zankl, C., Hutter, E., Unterluggauer, H., Laun, P., Heeren, G., Bogengruber, E., Herndler-Brandstetter, D., Breitenbach, M. and Jansen-Durr, P. (2007) Partial uncoupling of oxidative

phosphorylation induces premature senescence in human fibroblasts and yeast mother cells. Free radical biology & medicine. **43**, 947-958

16 Passos, J. F., Saretzki, G., Ahmed, S., Nelson, G., Richter, T., Peters, H., Wappler, I., Birket, M. J., Harold, G., Schaeuble, K., Birch-Machin, M. A., Kirkwood, T. B. and von Zglinicki, T. (2007) Mitochondrial dysfunction accounts for the stochastic heterogeneity in telomere-dependent senescence. PLoS Biol. **5**, e110

17 Jendrach, M., Pohl, S., Voth, M., Kowald, A., Hammerstein, P. and Bereiter-Hahn, J. (2005) Morpho-dynamic changes of mitochondria during ageing of human endothelial cells. Mechanisms of ageing and development. **126**, 813-821

18 Hutter, E., Unterluggauer, H., Garedew, A., Jansen-Durr, P. and Gnaiger, E. (2006) High-resolution respirometry--a modern tool in aging research. Experimental gerontology. **41**, 103-109

19 Babior, B. M., Lambeth, J. D. and Nauseef, W. (2002) The neutrophil NADPH oxidase. Archives of biochemistry and biophysics. **397**, 342-344

20 Krause, K. H. (2004) Tissue distribution and putative physiological function of NOX family NADPH oxidases. Jpn J Infect Dis. **57**, S28-29

21 Torres, M. and Forman, H. J. (2003) Redox signaling and the MAP kinase pathways. Biofactors. **17**, 287-296

22 Schroder, K., Helmcke, I., Palfi, K., Krause, K. H., Busse, R. and Brandes, R. P. (2007) Nox1 mediates basic fibroblast growth factor-induced migration of vascular smooth muscle cells. Arteriosclerosis, thrombosis, and vascular biology. **27**, 1736-1743

23 Brandes, R. P. (2003) Role of NADPH oxidases in the control of vascular gene expression. Antioxidants & redox signaling. **5**, 803-811

24 Gorin, Y., Ricono, J. M., Wagner, B., Kim, N. H., Bhandari, B., Choudhury, G. G. and Abboud, H. E. (2004) Angiotensin II-induced ERK1/ERK2 activation and protein synthesis are redox-dependent in glomerular mesangial cells. Biochem J. **381**, 231-239

25 Li, J., Stouffs, M., Serrander, L., Banfi, B., Bettiol, E., Charnay, Y., Steger, K., Krause, K. H. and Jaconi, M. E. (2006) The NADPH oxidase NOX4 drives cardiac differentiation: Role in regulating cardiac transcription factors and MAP kinase activation. Mol Biol Cell. **17**, 3978-3988

26 Mochizuki, T., Furuta, S., Mitsushita, J., Shang, W. H., Ito, M., Yokoo, Y., Yamaura, M., Ishizone, S., Nakayama, J., Konagai, A., Hirose, K., Kiyosawa, K. and Kamata, T. (2006) Inhibition of NADPH oxidase 4 activates apoptosis via the AKT/apoptosis signal-regulating kinase 1 pathway in pancreatic cancer PANC-1 cells. Oncogene. **25**, 3699-3707

27 Petry, A., Djordjevic, T., Weitnauer, M., Kietzmann, T., Hess, J. and Gorlach, A. (2006) NOX2 and NOX4 mediate proliferative response in endothelial cells. Antioxidants & redox signaling. **8**, 1473-1484

28 Li, S., Tabar, S. S., Malec, V., Eul, B. G., Klepetko, W., Weissmann, N., Grimminger, F., Seeger, W., Rose, F. and Hanze, J. (2008) NOX4 regulates ROS levels under normoxic and hypoxic conditions, triggers proliferation, and inhibits apoptosis in pulmonary artery adventitial fibroblasts. Antioxidants & redox signaling. **10**, 1687-1698

29 Mofarrahi, M., Brandes, R. P., Gorlach, A., Hanze, J., Terada, L. S., Quinn, M. T., Mayaki, D., Petrof, B. and Hussain, S. N. (2008) Regulation of proliferation of skeletal muscle precursor cells by NADPH oxidase. Antioxidants & redox signaling. **10**, 559-574

30 Brandes, R. P. and Schroder, K. (2008) Composition and functions of vascular nicotinamide adenine dinucleotide phosphate oxidases. Trends Cardiovasc Med. **18**, 15-19

31 Unterluggauer, H., Hutter, E., Voglauer, R., Grillari, J., Voth, M., Bereiter-Hahn, J., Jansen-Durr, P. and Jendrach, M. (2007) Identification of cultivation-independent markers of human endothelial cell senescence in vitro. Biogerontology. **8**, 383-397

32 Muck, C., Micutkova, L., Zwerschke, W. and Jansen-Durr, P. (2008) Role of insulin-like growth factor binding protein-3 in human umbilical vein endothelial cell senescence. Rejuvenation research. **11**, 449-453

33 Struthers, L., Patel, R., Clark, J. and Thomas, S. (1998) Direct detection of 8-oxodeoxyguanosine and 8-oxoguanine by avidin and its analogues. Analytical biochemistry. **255**, 20-31

34 Kinner, A., Wu, W., Staudt, C. and Iliakis, G. (2008) Gamma-H2AX in recognition and signaling of DNA double-strand breaks in the context of chromatin. Nucleic acids research. **36**, 5678-5694

35 Fehrer, C., Voglauer, R., Wieser, M., Pfister, G., Brunauer, R., Cioca, D., Grubeck-Loebenstein, B. and Lepperdinger, G. (2006) Techniques in gerontology: cell lines as standards for telomere length and telomerase activity assessment. Experimental gerontology. **41**, 648-651

36 Kawahara, T., Ritsick, D., Cheng, G. and Lambeth, J. D. (2005) Point mutations in the proline-rich region of p22phox are dominant inhibitors of Nox1- and Nox2-dependent reactive oxygen generation. The Journal of biological chemistry. **280**, 31859-31869

37 Rinaldi, M., Moroni, P., Paape, M. J. and Bannerman, D. D. (2007) Evaluation of assays for the measurement of bovine neutrophil reactive oxygen species. Vet Immunol Immunopathol. **115**, 107-125

38 Dikalov, S. I., Dikalova, A. E., Bikineyeva, A. T., Schmidt, H. H., Harrison, D. G. and Griendling, K. K. (2008) Distinct roles of Nox1 and Nox4 in basal and angiotensin II-stimulated superoxide and hydrogen peroxide production. Free radical biology & medicine. **45**, 1340-1351

39 Nauseef, W. M. (2008) Biological roles for the NOX family NADPH oxidases. The Journal of biological chemistry. **283**, 16961-16965

40 Hunte, C. e., von Jagow, G. e. and Schagger, H. e. (2003) Membrane Protein Purification and Crystallization: A Practical Guide, Second Edition. Elsevier Science (USA), New York

41 Chen, Q. M. (2000) Replicative senescence and oxidant-induced premature senescence. Beyond the control of cell cycle checkpoints. Ann N Y Acad Sci. **908**, 111-125.

42 Hultdin, M., Gronlund, E., Norrback, K., Eriksson-Lindstrom, E., Just, T. and Roos, G. (1998) Telomere analysis by fluorescence in situ hybridization and flow cytometry. Nucleic acids research. **26**, 3651-3656

43 Voglauer, R., Chang, M. W., Dampier, B., Wieser, M., Baumann, K., Sterovsky, T., Schreiber, M., Katinger, H. and Grillari, J. (2006) SNEV overexpression extends the life span of human endothelial cells. Experimental cell research. **312**, 746-759

44 Nystrom, T. (2005) Role of oxidative carbonylation in protein quality control and senescence. The EMBO journal. **24**, 1311-1317

45 Bartek, J. and Lukas, J. (2007) DNA damage checkpoints: from initiation to recovery or adaptation. Current opinion in cell biology. **19**, 238-245

46 d'Adda di Fagagna, F. (2008) Living on a break: cellular senescence as a DNA-damage response. Nature reviews. **8**, 512-522

47 Li, J. M. and Shah, A. M. (2002) Intracellular localization and preassembly of the NADPH oxidase complex in cultured endothelial cells. The Journal of biological chemistry. **277**, 19952-19960

48 Ushio-Fukai, M., Alexander, R. W., Akers, M. and Griendling, K. K. (1998) p38 Mitogen-activated protein kinase is a critical component of the redox-sensitive signaling pathways activated by

angiotensin II. Role in vascular smooth muscle cell hypertrophy. The Journal of biological chemistry. **273**, 15022-15029

49 Viedt, C., Soto, U., Krieger-Brauer, H. I., Fei, J., Elsing, C., Kubler, W. and Kreuzer, J. (2000) Differential activation of mitogen-activated protein kinases in smooth muscle cells by angiotensin II: involvement of p22phox and reactive oxygen species. Arteriosclerosis, thrombosis, and vascular biology. **20**, 940-948

50 Geiszt, M., Kopp, J. B., Varnai, P. and Leto, T. L. (2000) Identification of renox, an NAD(P)H oxidase in kidney. Proceedings of the National Academy of Sciences of the United States of America. **97**, 8010-8014

51 Imanishi, T., Hano, T. and Nishio, I. (2005) Angiotensin II accelerates endothelial progenitor cell senescence through induction of oxidative stress. Journal of hypertension. **23**, 97-104

52 Yao, E. H., Fukuda, N., Matsumoto, T., Kobayashi, N., Katakawa, M., Yamamoto, C., Tsunemi, A., Suzuki, R., Ueno, T. and Matsumoto, K. (2007) Losartan improves the impaired function of endothelial progenitor cells in hypertension via an antioxidant effect. Hypertens Res. **30**, 1119-1128

53 Schilder, Y. D., Heiss, E. H., Schachner, D., Ziegler, J., Reznicek, G., Sorescu, D. and Dirsch, V. M. (2009) NADPH oxidases 1 and 4 mediate cellular senescence induced by resveratrol in human endothelial cells. Free radical biology & medicine

FIGURE LEGENDS

Fig.1. Nox4 expression and activity in young and senescent HUVEC
A. HUVEC from four different donors were grown into senescence. RNA was prepared at early (y) and late (sen) passages and analyzed for expression of Nox4 by RT-PCR (upper panel) and qPCR (lower panel). Bar graphs represent mean values ± SD of three independent experiments.
B. Cells of HUVEC strain #1 were analyzed for ROS production by measurement of luminol-enhanced chemiluminescence at early passage (passage 7) and at senescence (passage 25), as indicated. 20 minutes after onset of the experiment, DPI (10 μM) was added to specifically inhibit NADPH oxidase activity. Bar graphs represent mean values ± SD of three independent experiments.

Fig. 2**.** Depletion of Nox4 abrogates ROS production in HUVEC
A. Young HUVEC of strains #1 and #3 were infected with lentiviral particles harbouring control shRNA or Nox4-specific shRNA, as indicated. 42 days after infection, RNA was prepared and Nox4 expression was analyzed by qPCR, using PBGD as normalization control. Fold change of Nox4 mRNA level is indicated, shown are the results of three independent experiments.
B. Validation of Nox4 knockdown by luminol-enhanced chemiluminescence. Cells were grown as described for panel A and ROS production was determined by applying luminol-enhanced chemiluminescence. The relative rate of ROS production is shown, comparing Nox4-knockdown cells and cells expressing control shRNA. Bar graphs represent mean values ± SD of three independent experiments.

Fig. 3. Depletion of Nox4 enhances cell proliferation
A. Young HUVEC of strain #1 and #3 were infected with lentiviral particles harbouring control shRNA or Nox4-specific shRNA. 42 days after infection, the proliferation rate was determined by BrdU incorporation experiments. The number of BrdU-positive cells was assessed as described in *Experimental*. The results are separately depicted for HUVEC strains #1 and #3, each case implicating three independent experiments.
B. Cells of HUVEC strains #1 and #3 were treated as described for panel A. 42 days after infection, cells were harvested. Cellular extracts were subjected to SDS-page and analyzed by Western blot analysis using antibodies to ERK, phospho-ERK, JNK, phoshpo-JNK, p38 and phospho-p38, as indicated. The quality of phospho-antibodies was evaluated using extracts of human fibroblasts that were either serum-starved for 72h, stimulated with 10% FCS (10 min), or treated with anisomycin (100nM, 20 min), respectively. Expression levels and phosphorylation status of ERK, JNK, and p38 was analyzed in three independent experiments; shown here are results of one representative experiment.
C. Results from three independent experiments, as described in panel B, were evaluated by densitometric and statistical analysis. Thereby the signal for phosphorylated protein was normalized to the signal intensity of the corresponding unphosphorylated form . Shown here are mean values (+/- SE) for HUVEC strains #1 and #3, as indicated. N.S.: non significant.

Fig. 4. Depletion of Nox4 delays the onset of replicative senescence
A. Cells of HUVEC strains #1 and #3 were infected with lentiviral particles, harbouring either control shRNA or Nox4-specific shRNA. RNA was prepared 110 days after infection (for strain #3) and 30 days after infection (for strain #1), respectively. The expression level of Nox4 was determined by qPCR. The fold regulation of Nox4 is shown in either case, bar graphs represent mean values ± SD of three independent experiments.
B. Cells of HUVEC strain #1 were treated as described for panel A and grown for 100 days after infection. Cells were passaged at regular intervals and thereby counted. Cell numbers were used to establish a growth curve, displaying cumulated population doublings. Cells were counted in three independent parallels. Standard deviations are indicated by error bars.
C. Cells of HUVEC strain #3 were treated as described for panel A and grown for 110 days after infection. Cells were passaged at regular intervals and thereby counted. Cell numbers were used to establish a growth curve, displaying cumulative population doublings. Cells were counted in three independent parallels. Standard deviations are indicated by error bars.
D. At 110 days post-infection, cells of HUVEC strain #3 (treated as described for panel A) were stained for presence of SA-ß-gal activity. Bars indicate the relative percentage of ß-gal-positive cells (± SD), results were derived from three independent experiments.

Fig. 5. Depletion of Nox4 enhances telomere shortening
Cells of HUVEC strains #1 and #3 infected with lentiviral particles, harbouring either control shRNA or Nox4-specific shRNA, were analyzed at passage 17 (HUVEC strain #1) or at passage 15 (HUVEC strain #3), as indicated. Telomere length was determined by Flow FISH technique as described in *Experimental*, using telomeres of TCL 1301 cells as a size marker. In each case, the calculated mean telomere length is indicated.

Fig. 6. Depletion of Nox4 prevents DNA damage
The degree of DNA damage was determined by quantification of 8-oxodeoxyguanosine (8 oxo-dG; panel A) and histone variant γ–H2AX (panels B, C).
A. Cells of HUVEC strains #1 and #3 (p5) were infected with lentiviral particles harbouring control shRNA and Nox4-specific shRNA, respectively. At passage 23 (strain #1) and passage 22 (strain #3), respectively, cells were stained with avidin-FITC. Fluorescence intensity was analyzed by flow cytometry. As a negative control, cells incubated in the absence of avidin-conjugated FITC were used. Shown here is the histogram of one representative experiment (n = 3).
B. HUVEC strain #3 was infected with control shRNA or Nox4-specific shRNA at passage 5. At passage 26, cells were stained using indirect immunofluorescence and anti-γ-H2AX primary antibody. Cells incubated for 1h at room temperature with 100 μM H_2O_2 in HBSS were used as positive control. As negative control, primary antibody was omitted. Samples were analyzed using confocal microscopy.
C. HUVEC strains #1 and #3 (p5) were infected with either control shRNA or Nox4-specific shRNA, and stained as described for panel B. Staining was performed at passage 23 (strain #1) and passage 22 (strain #3), respectively. Shown here is the histogram of one representative experiment (n = 3).

Biochemical Journal Immediate Publication. Published on 14 Aug 2009 as manuscript BJ20090666

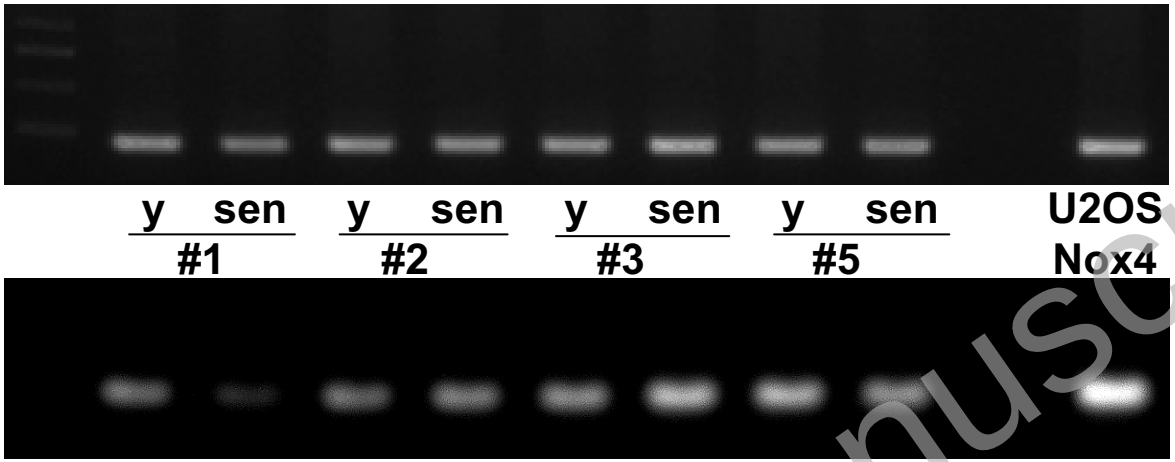

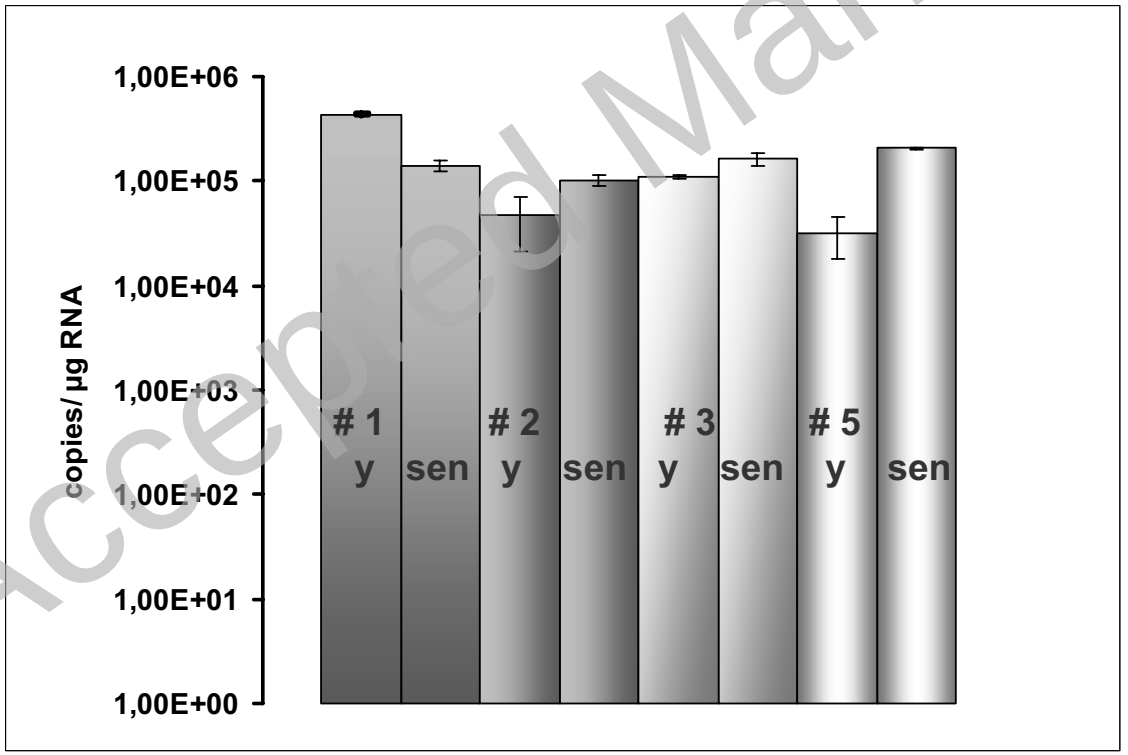

Fig. 1A

Biochemical Journal Immediate Publication. Published on 14 Aug 2009 as manuscript BJ20090666

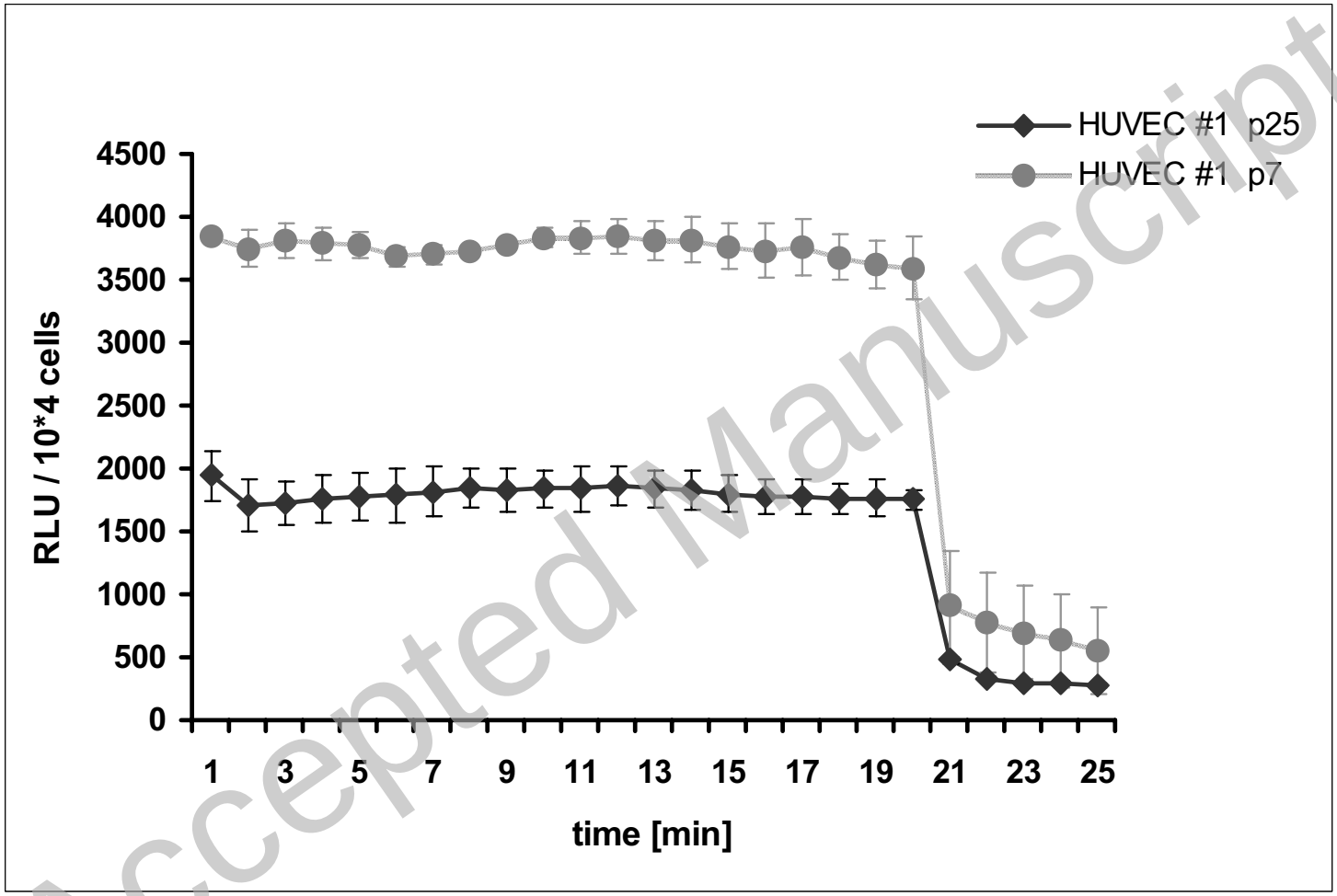

Fig. 1B

Biochemical Journal Immediate Publication. Published on 14 Aug 2009 as manuscript BJ20090666

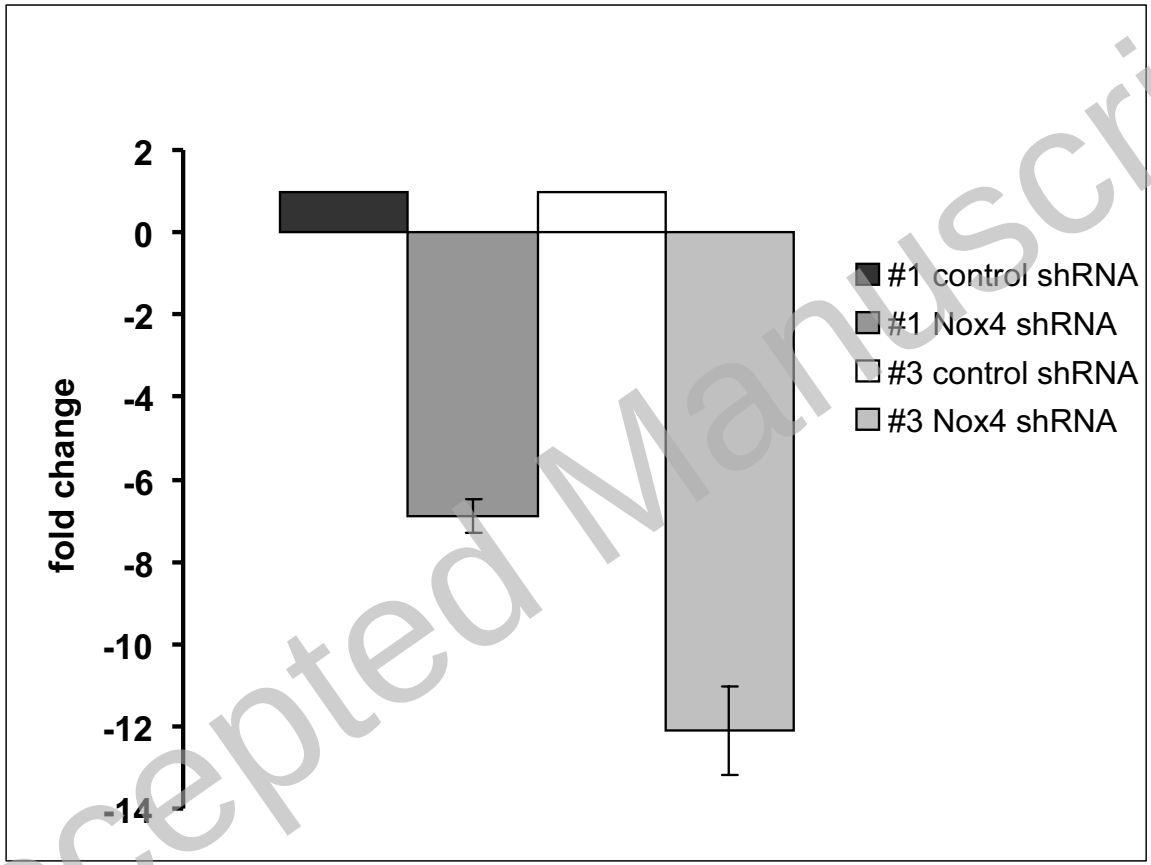

Fig. 2A

Biochemical Journal Immediate Publication. Published on 14 Aug 2009 as manuscript BJ20090666

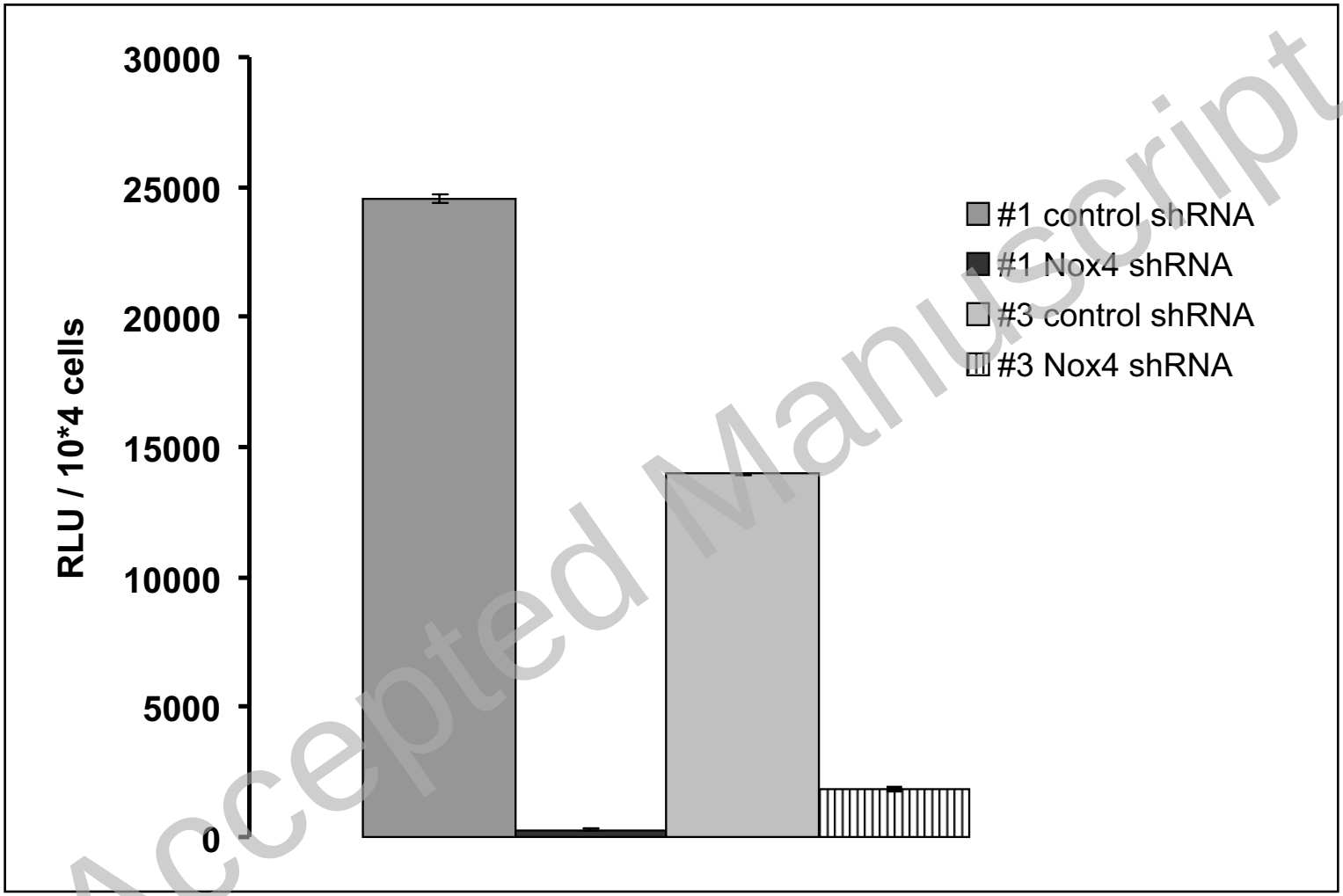

Fig. 2B

Biochemical Journal Immediate Publication. Published on 14 Aug 2009 as manuscript BJ20090666

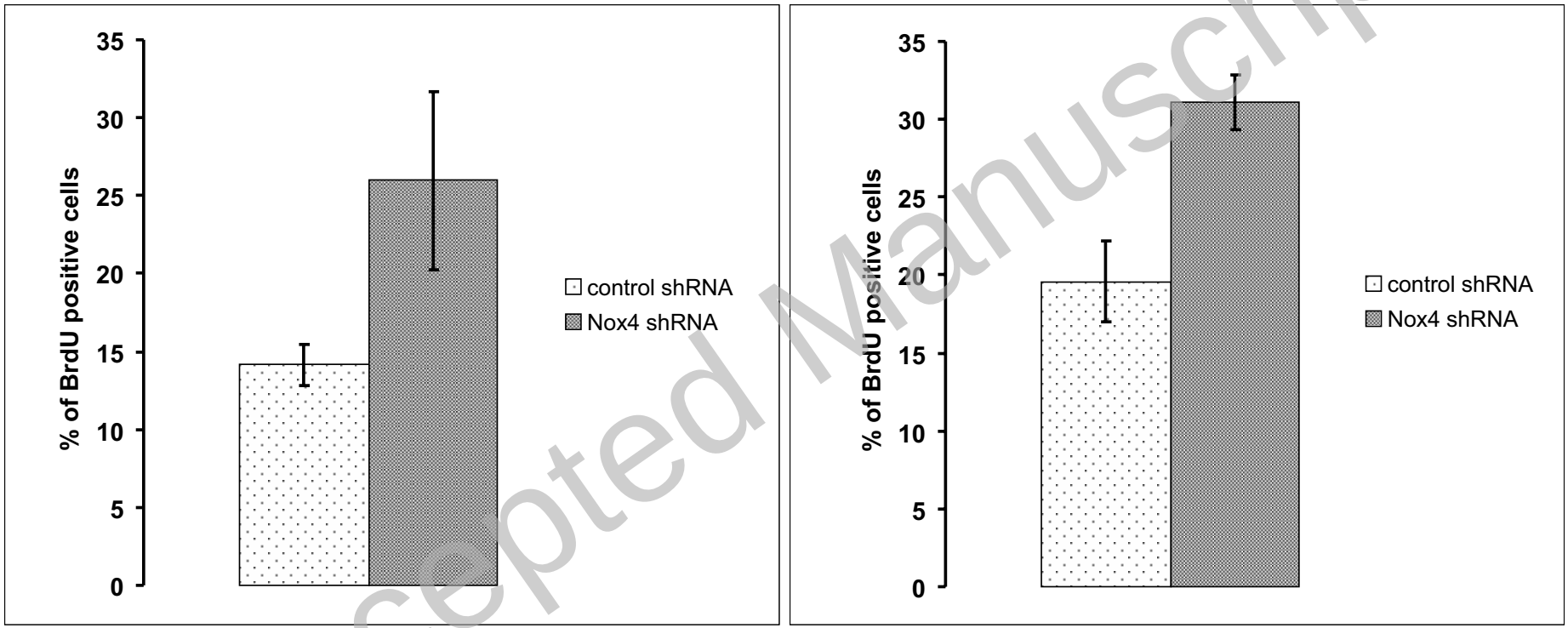

Fig. 3A

Biochemical Journal Immediate Publication. Published on 14 Aug 2009 as manuscript BJ20090666

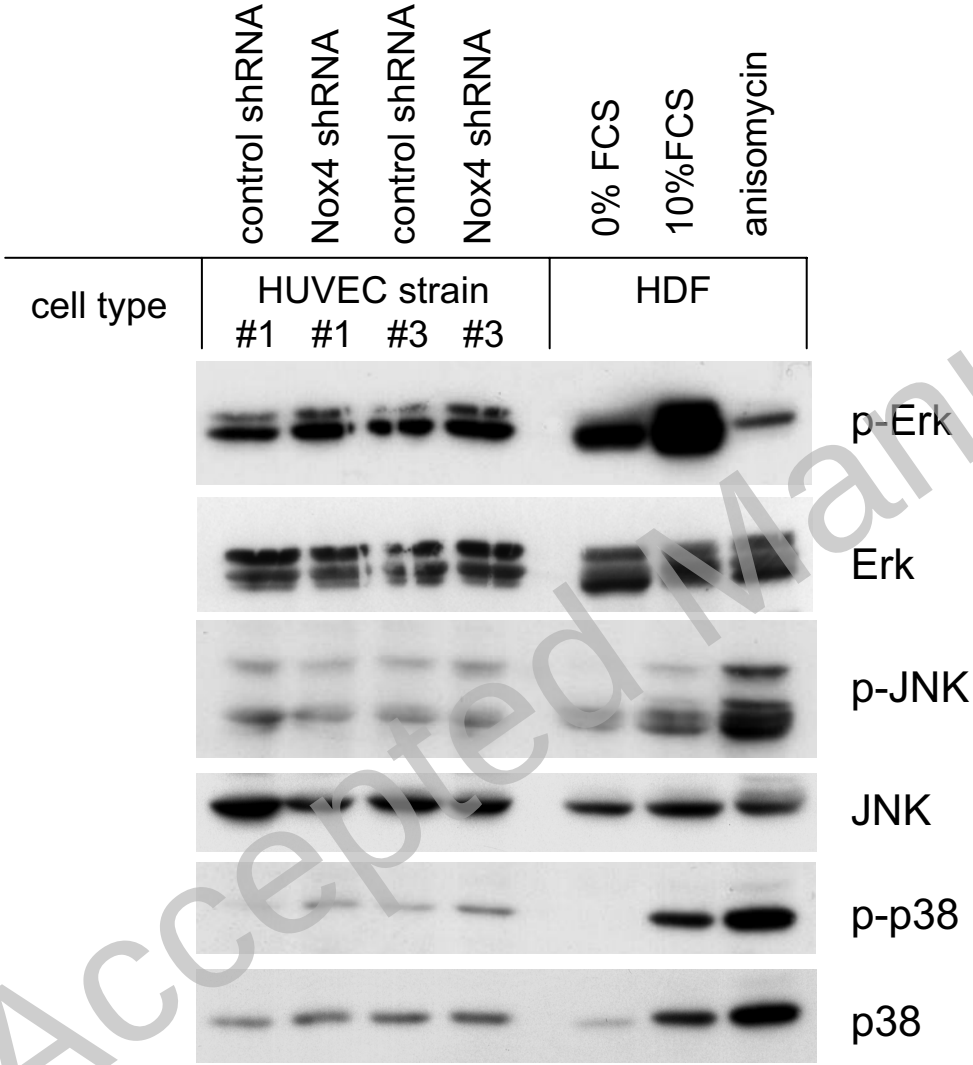

Fig. 3B

Biochemical Journal Immediate Publication. Published on 14 Aug 2009 as manuscript BJ20090666

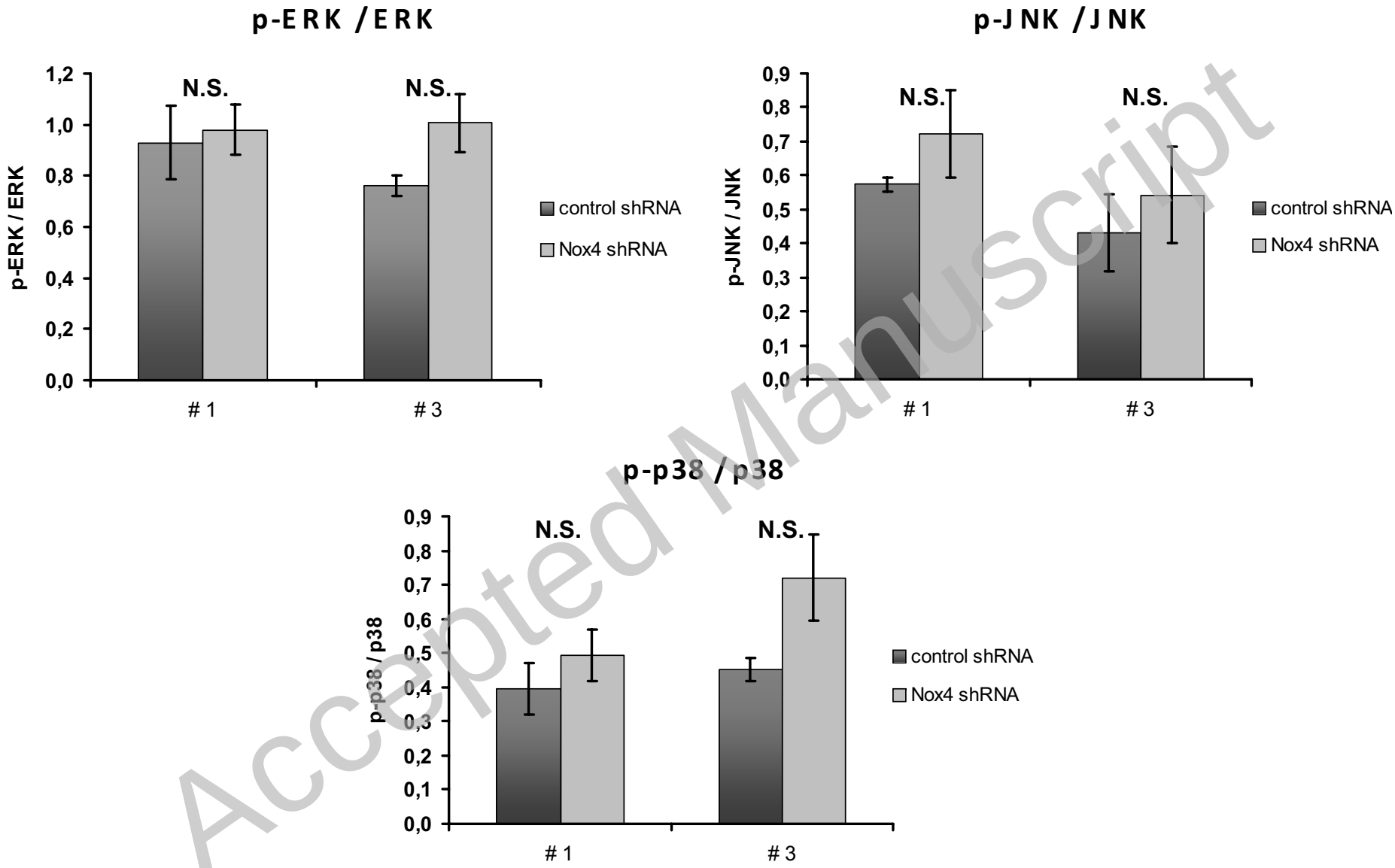

Fig. 3C

Biochemical Journal Immediate Publication. Published on 14 Aug 2009 as manuscript BJ20090666

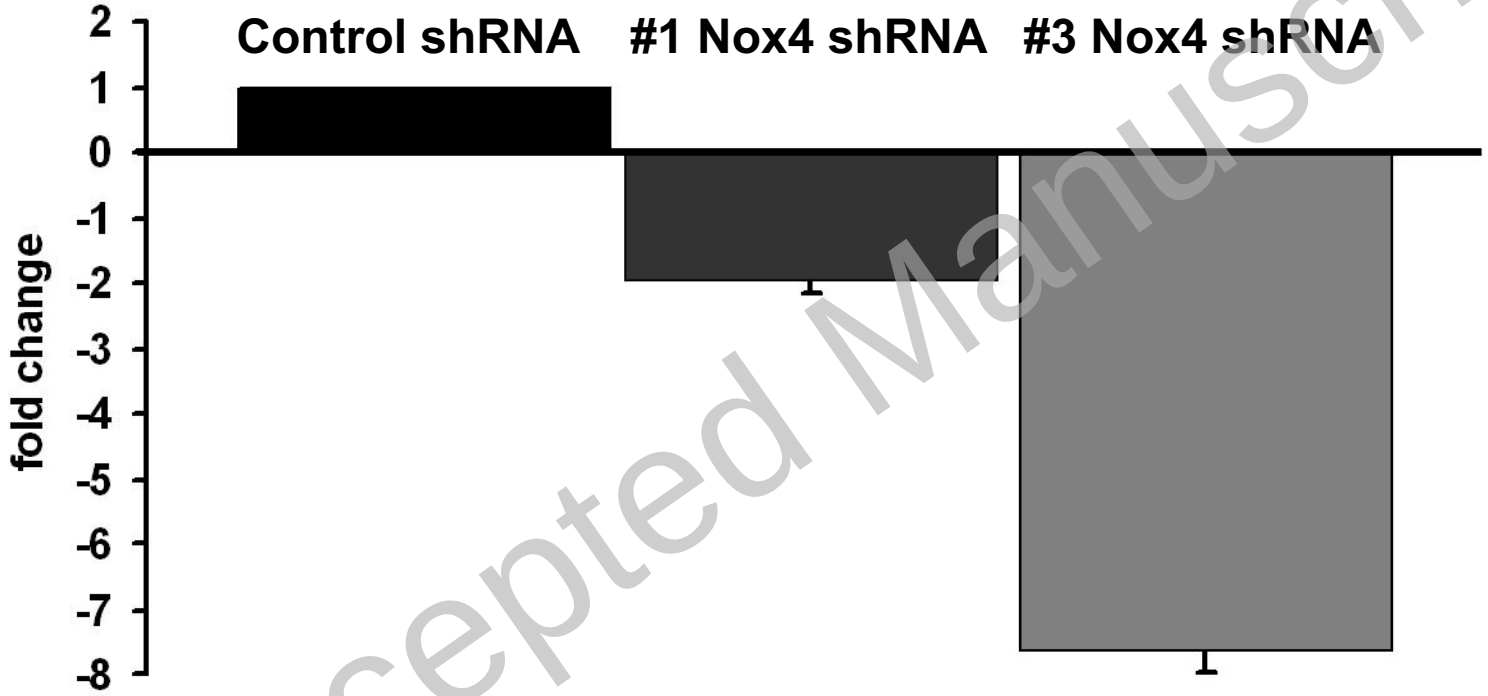

Fig. 4A

Biochemical Journal Immediate Publication. Published on 14 Aug 2009 as manuscript BJ20090666

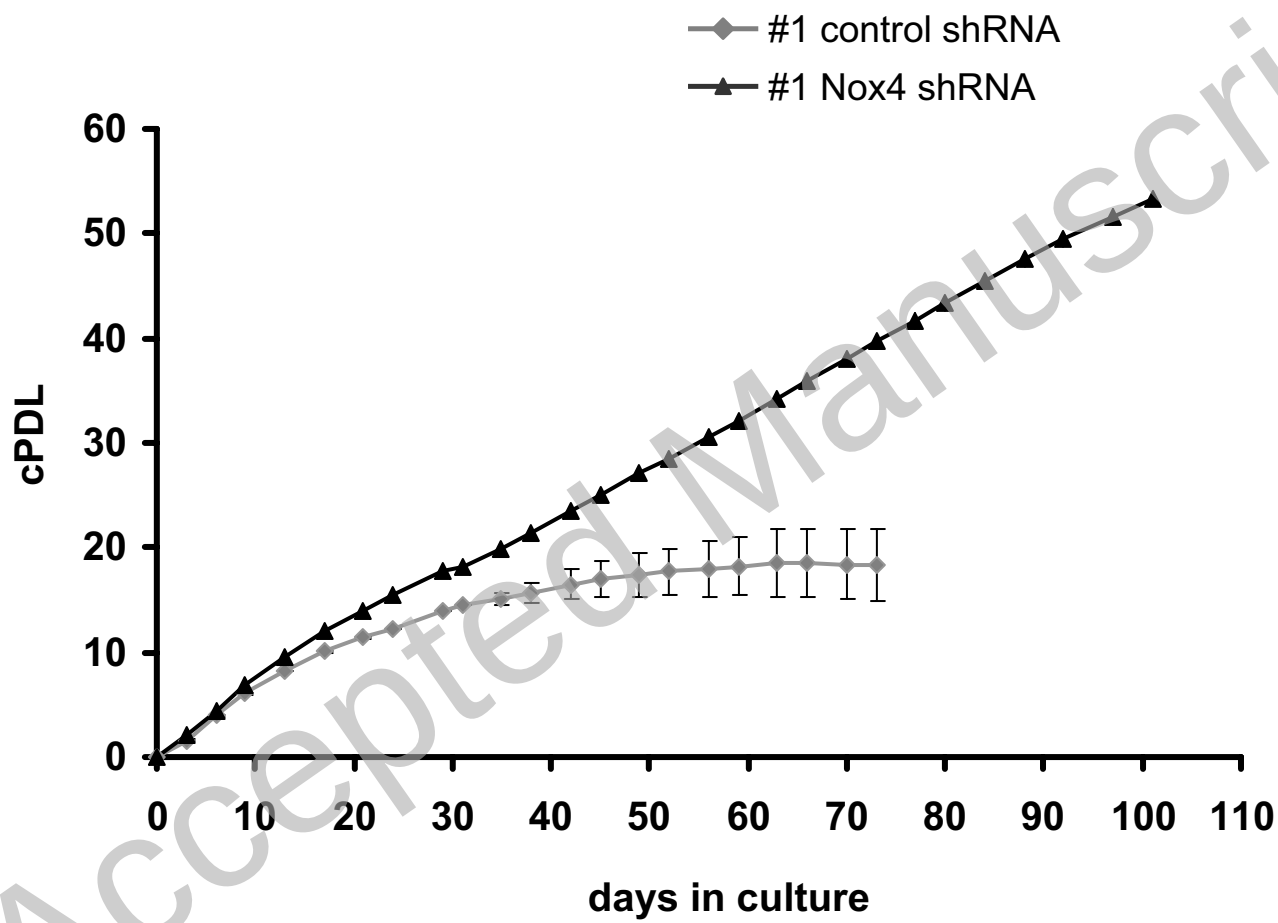

Fig. 4B

Biochemical Journal Immediate Publication. Published on 14 Aug 2009 as manuscript BJ20090666

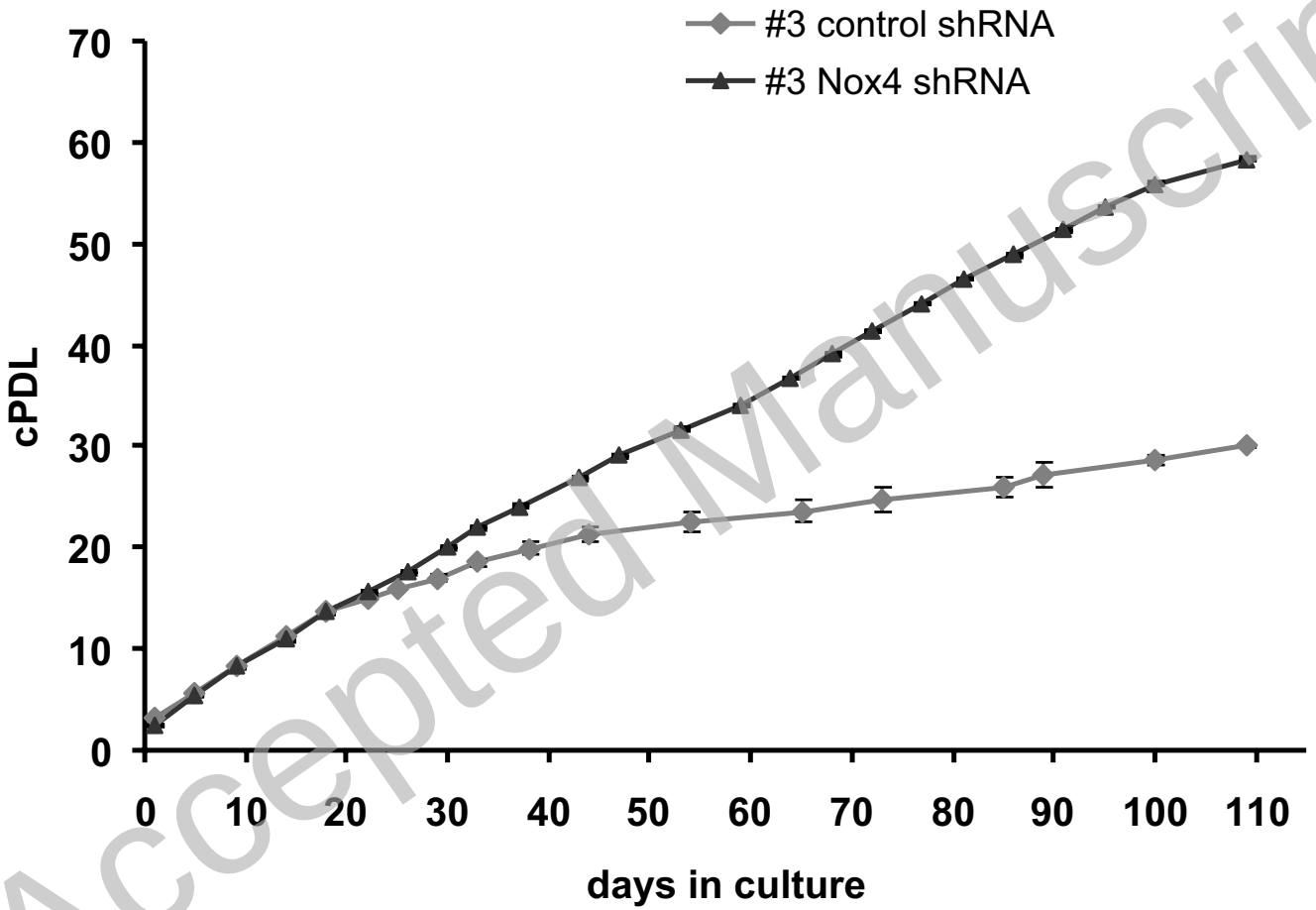

Fig. 4C

Biochemical Journal Immediate Publication. Published on 14 Aug 2009 as manuscript BJ20090666

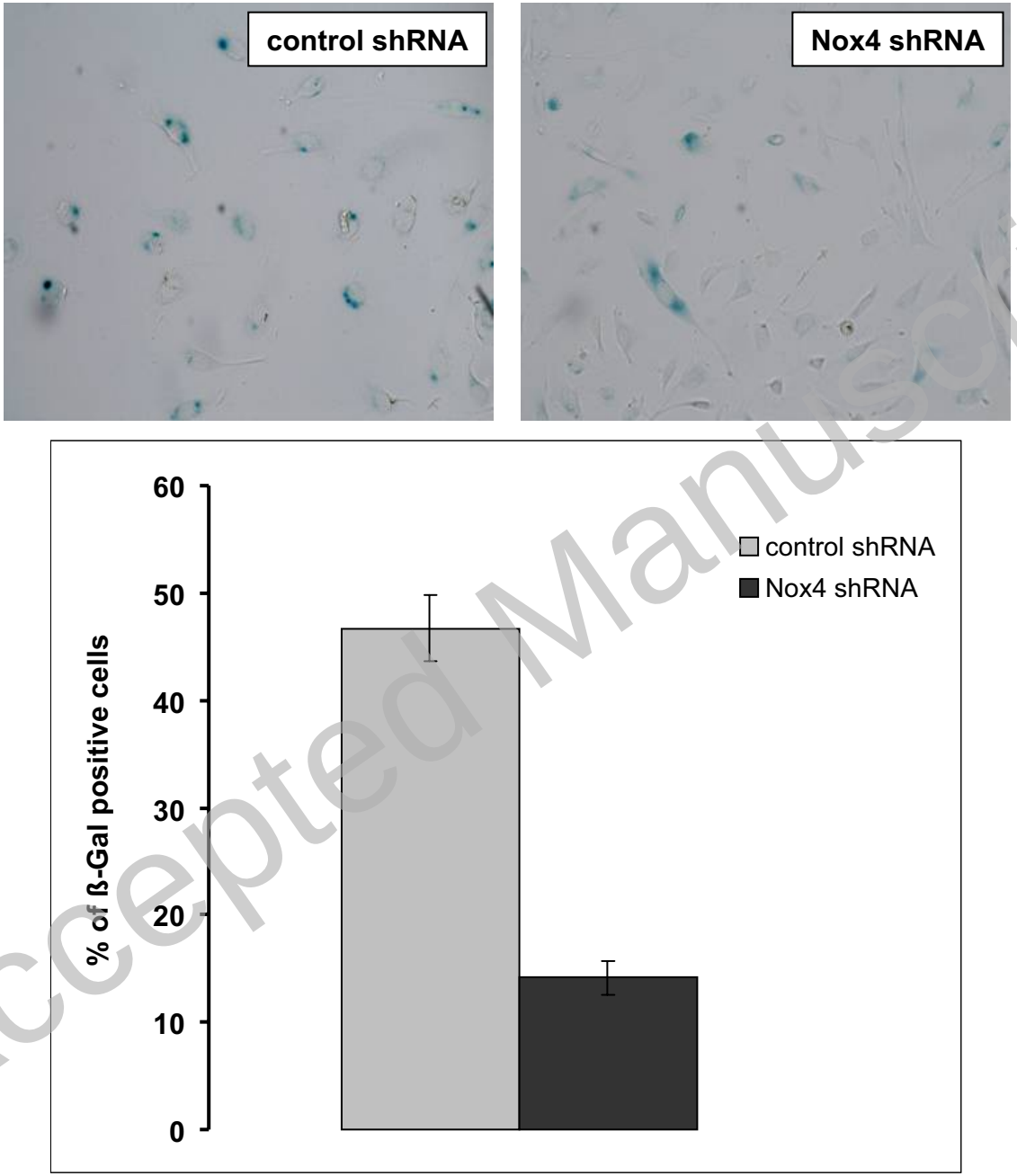

Fig. 4D

Biochemical Journal Immediate Publication. Published on 14 Aug 2009 as manuscript BJ20090666

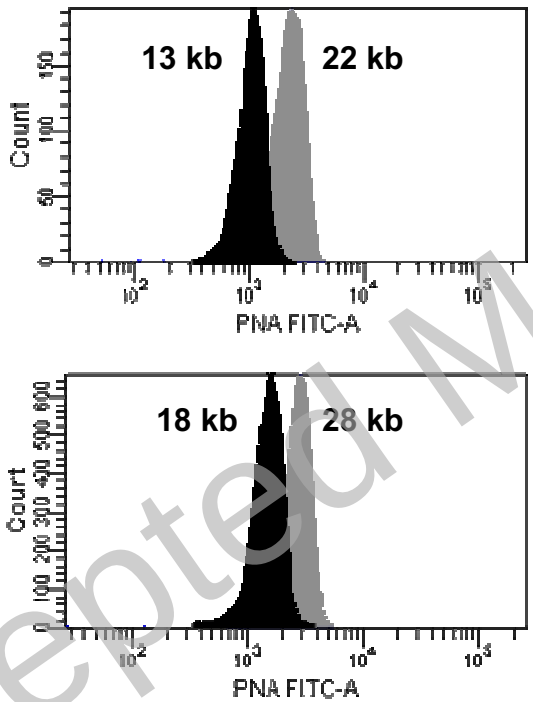

#3 control shRNA

#3 Nox4 shRNA

#1 control shRNA

#1 Nox4 shRNA

Fig. 5

Biochemical Journal Immediate Publication. Published on 14 Aug 2009 as manuscript BJ20090666

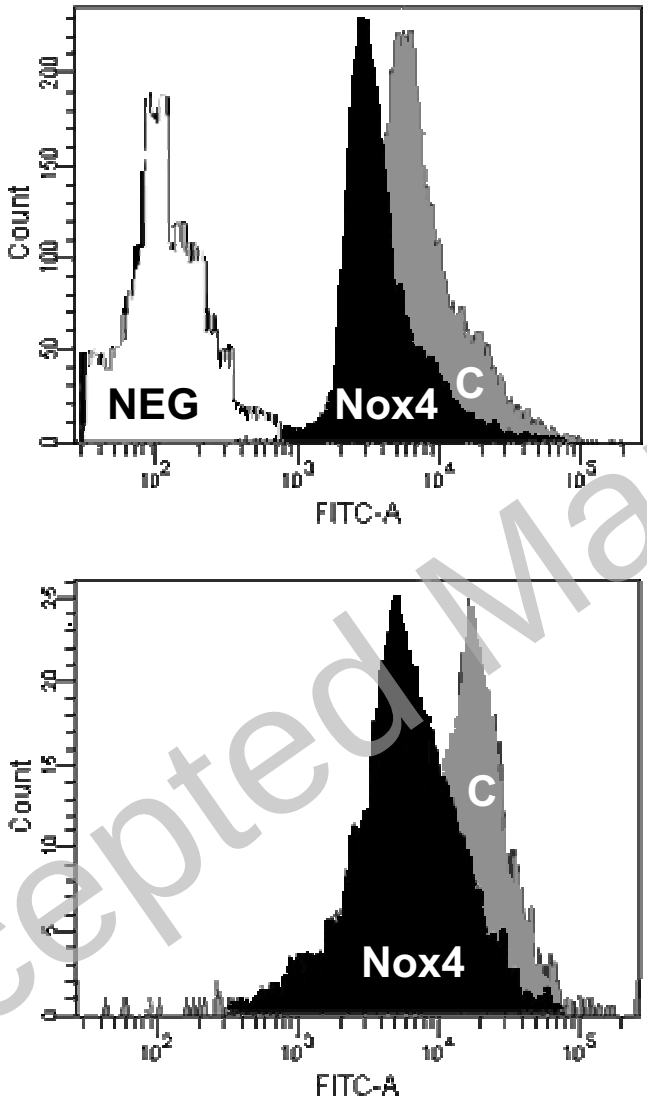

Fig. 6A

Biochemical Journal Immediate Publication. Published on 14 Aug 2009 as manuscript BJ20090666

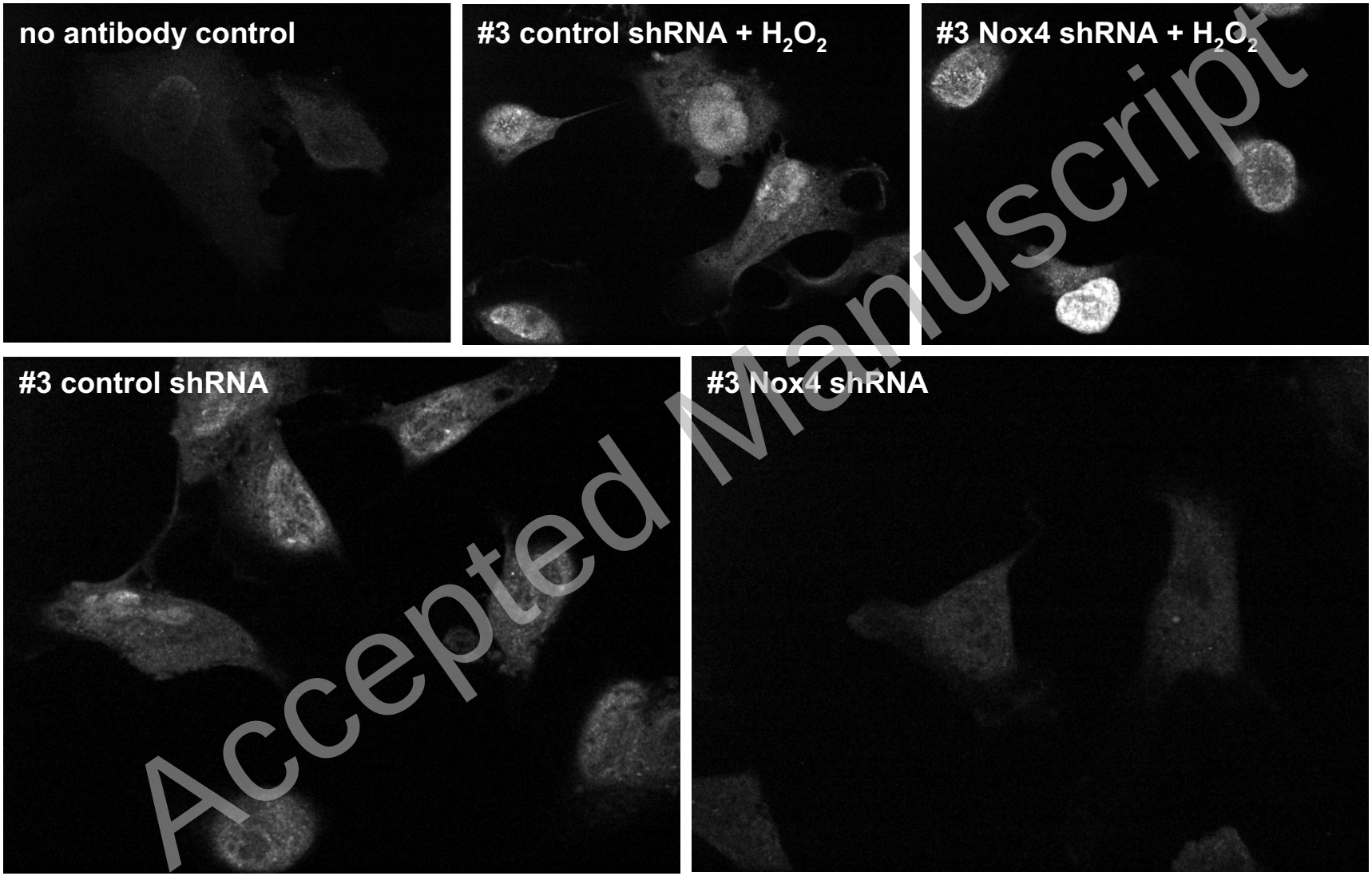

Fig. 6B

Biochemical Journal Immediate Publication. Published on 14 Aug 2009 as manuscript BJ20090666

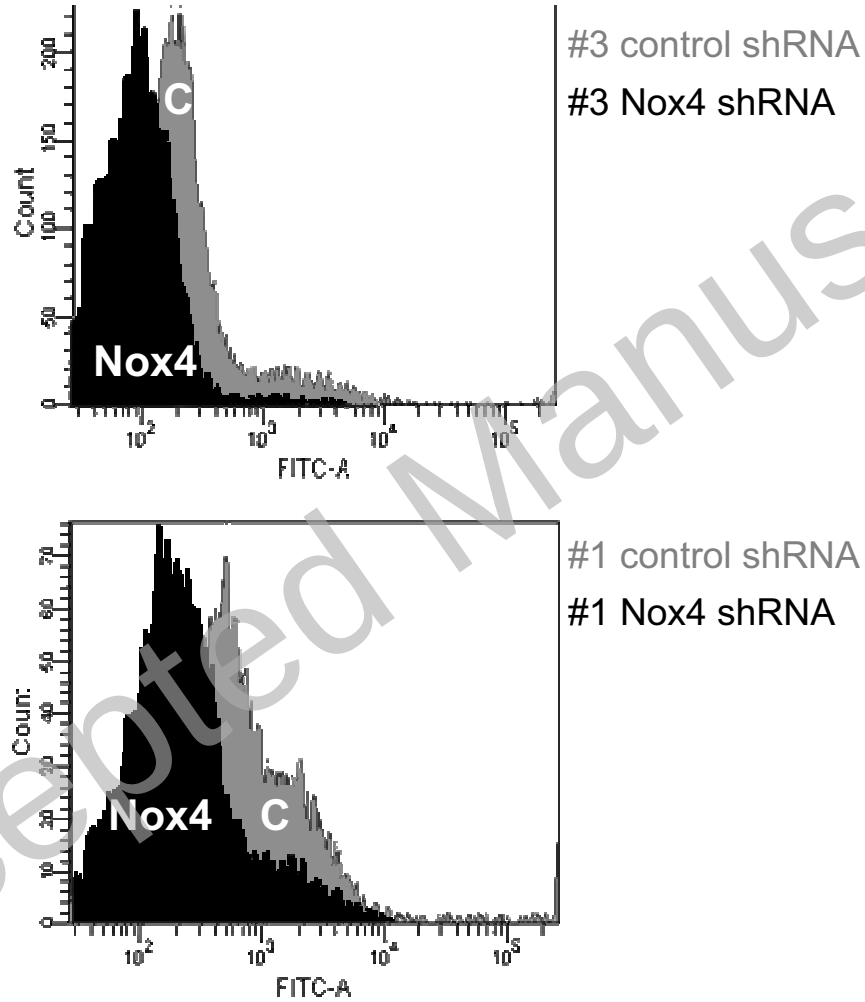

Fig. 6C